

AD-A119 151

TECHNICAL  
LIBRARY

AD

AD-E400 877

TECHNICAL REPORT ARLCD-CR-82039

ELECTRONIC JOINT ARMY/NAVY POINT DETONATING/DELAY FUZE

ALAN H. WENDLER  
HONEYWELL INC.  
5901 SOUTH COUNTY ROAD 18  
EDINA, MINNESOTA 55436

JOHN BIANCHI  
PROJECT ENGINEER  
ARRADCOM

August 1982



**US ARMY ARMAMENT RESEARCH AND DEVELOPMENT COMMAND**  
**LARGE CALIBER**  
**WEAPON SYSTEMS LABORATORY**  
**DOVER, NEW JERSEY**

Approved for public release; distribution unlimited.

SECURITY CLASSIFICATION OF THIS PAGE (WHEN DATA ENTERED)

REPORT DOCUMENTATION PAGE		READ INSTRUCTIONS BEFORE COMPLETING FORM
1. REPORT NUMBER ARLCD-CR-82039	2. GOV'T ACCESSION NUMBER	3. RECIPIENT'S CATALOG NUMBER
4. TITLE (AND SUBTITLE) ELECTRONIC JOINT ARMY/NAVY POINT DETONATING/DELAY FUZE		5. TYPE OF REPORT/PERIOD COVERED Final Report 21 July 1981 to 21 April 1982
		6. PERFORMING ORG. REPORT NUMBER
7. AUTHOR(S) Alan H. Wendler, Honeywell, Inc. John Bianchi, Project Engr, ARRADCOM		8. CONTRACT OR GRANT NUMBER(S) DAAK10-81-C-0195
9. PERFORMING ORGANIZATIONS NAME/ADDRESS Honeywell, Inc. 5901 South County Road 18 Edina, Minnesota 55436		10. PROGRAM ELEMENT, PROJECT, TASK AREA & WORK UNIT NUMBERS
11. CONTROLLING OFFICE NAME/ADDRESS ARRADCOM, TSD STINFO Div (DRDAR-TSS) Dover, NJ 07801		12. REPORT DATE August 1982
		13. NUMBER OF PAGES 71
14. MONITORING AGENCY NAME/ADDRESS (IF DIFFERENT FROM CONT. OFF.) ARRADCOM, LCWSL Nuclear & Fuze Division (DRDAR-LCN-T) Dover, NJ 07801		15. SECURITY CLASSIFICATION (OF THIS REPORT) Unclassified
		15a. DECLASSIFICATION DOWNGRADING SCHEDULE
16. DISTRIBUTION STATEMENT (OF THIS REPORT)  Approved for public release; distribution unlimited.		
17. DISTRIBUTION STATEMENT (OF THE ABSTRACT ENTERED IN BLOCK 20, IF DIFFERENT FROM REPORT)		
18. SUPPLEMENTARY NOTES		
19. KEY WORDS (CONTINUE ON REVERSE SIDE IF NECESSARY AND IDENTIFY BY BLOCK NUMBER) electronic fuze                      revolution counter setback sensor                      low voltage detector revolution sensor                    impact sensor spin rate detector                    programmable feasibility		
20. ABSTRACT (CONTINUE ON REVERSE SIDE IF NECESSARY AND IDENTIFY BY BLOCK NUMBER)  This report describes the second exploratory development program Honeywell conducted on the Electronic JAN PD/D Fuze. The objective of this program was to design and evaluate the subsystem modules required for an Electronic JAN PD/D Fuze.		

HD-168 REV 11/74

## Contents

Section	Page
1 Introduction	1
2 Setback Sensor	2
3 Revolution Sensor	12
3.1 Spin Fixture	13
3.2 First Program Development	16
3.3 Second Program Development	18
4 Spin Rate Detector	26
5 Revolution Counter	28
6 Programmable Feasibility	29
7 Impact Sensor	33
8 Low Voltage Detector	36
9 Demonstrator	41
10 Power Supply Tasks	47
11 Electronic S&A	48
11.1 Explosive Barrier Module	49
11.2 Internal Development Program	51
12 Fuze Packaging	52
13 Conclusions	52
14 Recommendations	54
Appendixes	
A Piezoelectric Setback Sensor Program for a HP-41C	57
B PZ Voltage Table Program for the HP-41C	66
Distribution List	71

## List of Illustrations

Figure		Page
2-1	Setback Sensor and Signal Discriminator	3
2-2	Setback Test Assembly	7
2-3	JAN Setback Sensor vs Accelerometer	8
2-4	Integrated Setback Sensor Circuit	8
2-5	440 G Setback Data	10
2-6	466 G Setback Data	10
2-7	575 G Setback Data	11
2-8	639 G Setback Data	11
3-1	JAN Spin Fixture	15
3-2	Spin Rate Amplifier	17
3-3	Revolution Sensor Amplifier	19
3-4	Coil-Penetrator Test Orientation	23
4-1	Spin Rate Detector	27
7-1	Impact Super Quick/Auto Delay Circuit	34
8-1	Low Voltage Detector Test Circuit	39
8-2	3N170 LVD Data	40
8-3	3N171 LVD Data	40
9-1	Demonstrator	42
9-2	Demonstrator Setback Circuit	43
9-3	Demonstrator Revolution Sensor Circuit	45
9-4	Demonstrator Impact Circuit	46
11-1	Explosive Barrier Module	50
12-1	Electronic JAN PD/D Fuze	53

## List of Tables

Table		Page
2-1	Crystal Specifications	5
2-2	Prestress Test Data	9
3-1	Revolution Sensor Output vs Spin Rate	17
3-2	First Program Sensitivity Window Data	19
3-3	Coil Sensitivity vs Amplifier Voltage	22
3-4	Coil Penetrator vs Non-Penetrator Sensitivity Window	23
3-5	Pole Piece Sensitivity Data	25
6-1	Voltage Transfer Data 500T #37 Coils	31
6-2	Voltage Transfer Data 1000T #44 Coils	32

## 1. Introduction

This report describes the continued exploratory development program conducted by Honeywell on the Electronic Joint Army/Navy Point Detonating/Delay Fuze. Honeywell engineering, technician, drafting, and support personnel expended 1133 hours in a nine month period towards the design and evaluation of several sub-systems required for the Electronic JAN PD/D fuze.

Honeywell achieved excellent results in many program areas. The integrated shock tower system was constructed and used to document proper setback sensor performance. A revolution sensor task was completed which evaluated a high production magnetometer and several other revolution sensor candidates. This task resulted in the development of a new pole piece revolution sensor which has advantages over any other candidate studied. We developed a Low Voltage Detector to achieve fuze cleanup and a demonstrator model to demonstrate the environmental sensor operation. The model demonstrates the setback, revolution spin rate detector, revolution counter, and super quick or auto delay impact features used on the Electronic JAN PD/D fuze. Honeywell and Navy personnel conducted a programmable feasibility task which revealed additional development is needed before the Electronic JAN PD/D fuze revolution sensor can be used as a receiver link for a magnetically coupled Multi-Option fuze. Honeywell did not conduct power supply tests to demonstrate fuze feasibility due to Explosive Barrier Module program uncertainty and hardware limitations.

This report focuses on testing Honeywell completed during this program, but also includes a limited discussion of the previous effort we conducted under the initial exploratory program, contract number DAAK10-80-C-0049. We included the

Electronic S&A and Fuze Packaging sections to present a complete understanding of the overall Electronic Joint Army/Navy Point Detonating/Delay Fuze concept.

## 2. Setback Sensor

A piezoelectric transducer was chosen for the JAN PD/D fuze setback sensor because feasibility of this approach has been demonstrated by Honeywell's Electronic S&A Internal Development program. A piezoelectric crystal performs as a transducer by converting mechanical stress into an electrical impulse so a setback sensor can be constructed by placing a weight above a piezoelectric crystal and monitoring the crystal output. Setback acceleration causes the weight to stress the piezoelectric crystal which generates an output proportional to the setback acceleration encountered. Integration of the piezoelectric crystal output assures the setback force encountered is actually caused by gun launch and not a forty foot drop on concrete or random handling shock. Figure 2-1 shows a typical piezoelectric sensor and signal discriminator circuit with several waveforms to detail theoretical circuit operation. A load capacitor ( $C_L$ ) is placed in parallel with the piezoelectric crystal to decrease crystal output for large applied forces and a clipping diode is used to prevent large voltages from damaging the threshold detector circuit. A rectifying diode enables evaluation only of the important positive slope portion of the acceleration curve and the resistor controls the capacitor charging rate for integration of the piezoelectric crystal output.

The first waveform in Figure 2-1 shows the relatively short duration of an accidental drop on concrete compared to a valid setback acceleration curve. The second waveform shows how the clipping diode limits the voltages to 10 volts and

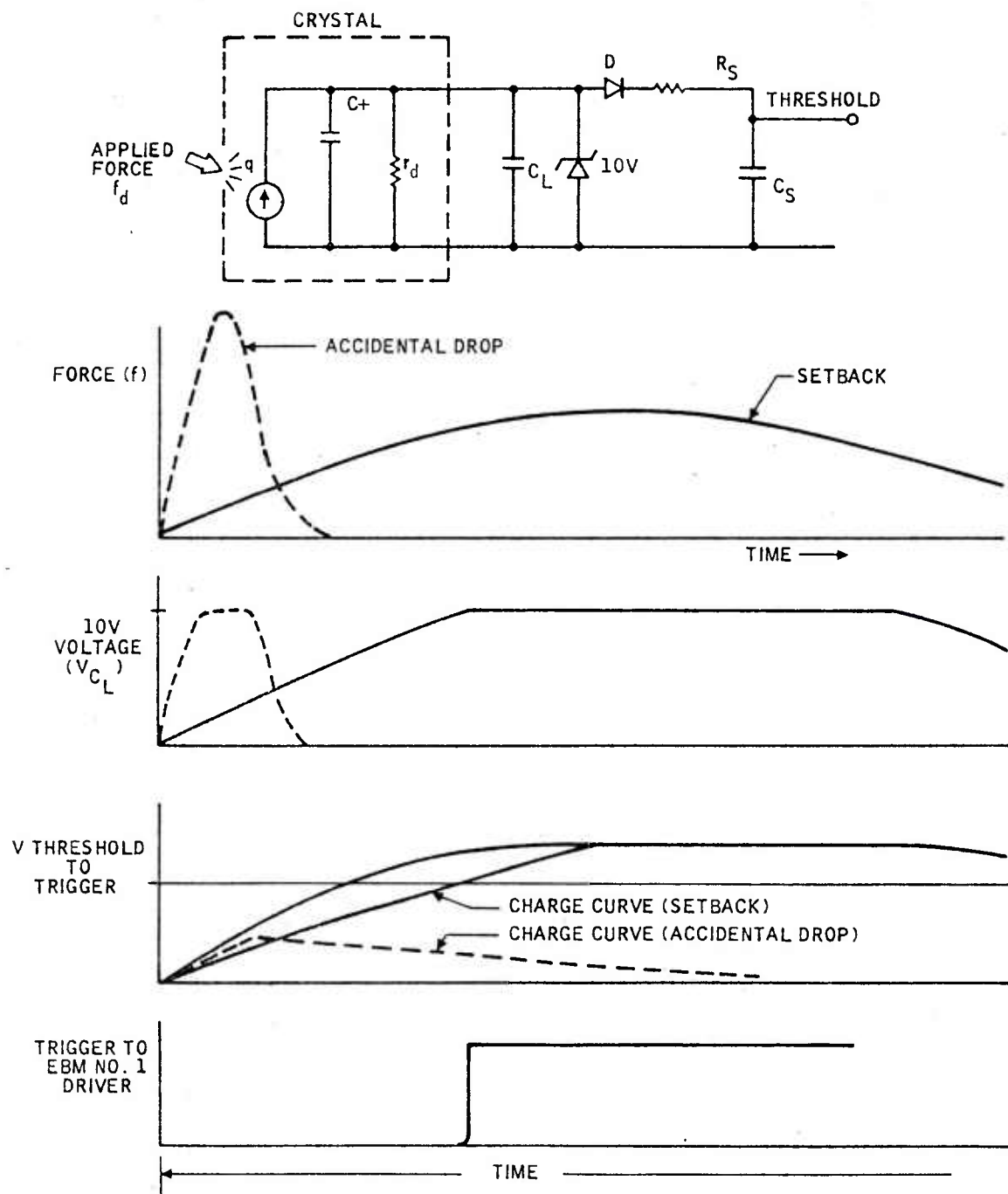


FIGURE 2-1. SETBACK SENSOR AND SIGNAL DISCRIMINATOR



the third waveform shows the setback and accidental drop charge curves in relation to the encountered setback acceleration curve. The accidental drop charge curve never reaches the required threshold to trigger due to short accidental drop pulse duration, but the setback charge curve reaches the required threshold and triggers the Explosive Barrier Module number 1 driver, as shown in waveform four. This demonstrates how the Honeywell designed signal discriminator rejects an accidental drop, but accepts a valid setback acceleration.

A piezoelectric crystal outputs a voltage which is related to several factors such as: crystal size, crystal sensitivity, setback weight, setback force, and external capacitance. A Piezoelectric Setback Sensor Program was written for a programmable HP-41C calculator to calculate the crystal output voltage given by equation 1. The calculator program and equation derivation are presented in Appendix A and Appendix B includes a voltage table program used to generate a table of output voltages for various setback accelerations and external load capacitances.

$$V_{out} = \frac{\frac{\pi(d_{pz})^2}{4} \times L_{wt} \times \rho_{wt} \times \text{setback} \times \left(\frac{9.80m}{sec^2}\right) \times \left(\frac{.4536 kg}{1b}\right) \times d_{33}}{\frac{\pi(d_{pz})^2 \times \epsilon_0 \times \left(\frac{2.54cm}{in}\right) + C_{ext}}{4 \times L_{pz}}}$$

The Army requirement for the JAN fuze is all arm at 600 g's and no arm at 400 g's; therefore the JAN signal discriminator must detect various amplitudes with similar pulse durations. For this application, the discriminator components are chosen so a 600 g setback pulse will produce a piezoelectric sensor output which will enable the integrator capacitor to charge above the threshold voltage while a 400 g setback pulse will not produce a piezoelectric sensor output sufficient

to charge the integrator capacitor to the threshold voltage. This will enable discrimination of various amplitude setback pulses and conformance to the specified JAN setback requirements.

The JAN setback sensor uses a C-16 type piezoelectric crystal (see Table 2-1 for specifications) 0.185" diameter x 0.125" length. The cylindrical shaped piezoelectric crystal is mounted with a 0.185" diameter x 0.100" long steel weight above it. Electrical connection to the piezoelectric crystal electrodes are made by a flexible circuit and the assembly is mounted in a fixture suitable for shock tower testing. A piezoelectric crystal is most sensitive when prestressed to 1500 psi, so Honeywell included a prestress screw in the fixture for this purpose. (An alternate method used on the Advanced Lightweight Torpedo program uses a C-spring assembly for prestressing the crystal.)

Table 2-1. Crystal Specifications

Material	C-16 Type 11 PZ-PT
Diameter	0.185 $\pm$ 0.002"
Thickness	0.125 $\pm$ 0.001"
Poling Direction	Through Thickness
$d_{33}$	400 pcoulomb/Newton

A signal discriminator for the JAN fuze was constructed and connected to a threshold detector which was powered by a 9V battery. When the threshold detector input exceeded the reference voltage, a latch was set which turned a LED on to indicate an accepted pulse. The output of the latch was connected to a monitor line so discriminator acceptance v.s. shock pulse could be recorded on an

oscilloscope. This data is valuable because it shows when the circuit sets for a particular shock pulse.

The JAN setback sensor, signal discriminator, display circuit, and battery were mounted to an aluminum plate and this integrated setback sensor, Figure 2-2, was mounted to the shock tower and tested. Before valid data could be collected, the piezoelectric crystal had to be prestressed to its sensitive operating point, as previously discussed. A torque wrench indirectly recorded the crystal prestress force since no direct method of measuring crystal prestress force was readily available. (This procedure was deemed adequate since the objective of this test was to demonstrate shock pulse differentiation, not accurate measurement of crystal prestress force.) The piezoelectric sensor output was connected directly to the threshold detector without an integrator. The time for the sensor output to reach an arbitrarily selected 3.9V reference level and turn the circuit on by setting the latch was recorded for various torques.

As can be seen from the data in Table 2-2, a torque applied to the prestress screw of zero or two inch pounds resulted in the setback sensor output reaching the 3.9V reference (and setting the latch) in 1.2m seconds. Increasing the applied torque to 6 or 8 inch pounds resulted in the latch setting in approximately 0.3m seconds, which indicated increased setback sensor sensitivity. The output of the JAN setback sensor without an integrator or threshold detector connected was compared to the output of the shock tower accelerometer, Figure 2-3, and the positive slope portion of the JAN sensor was sufficiently similar to the accelerometer positive slope portion therefore, testing was conducted with the setback sensor prestress screw torque equal to eight inch pounds.



FIGURE 2-2. SETBACK TEST ASSEMBLY



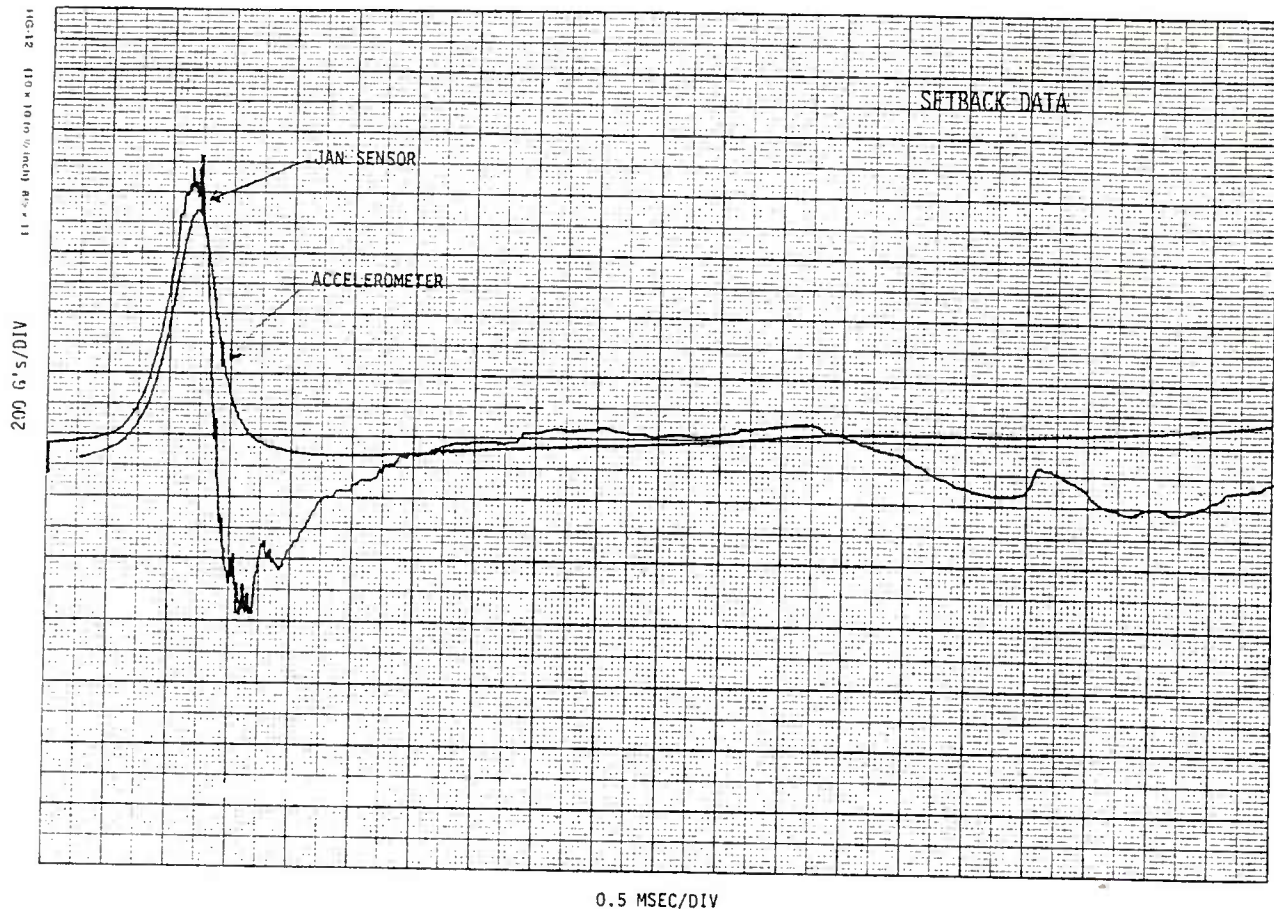


Figure 2-3 JAN sensor v.s. accelerometer

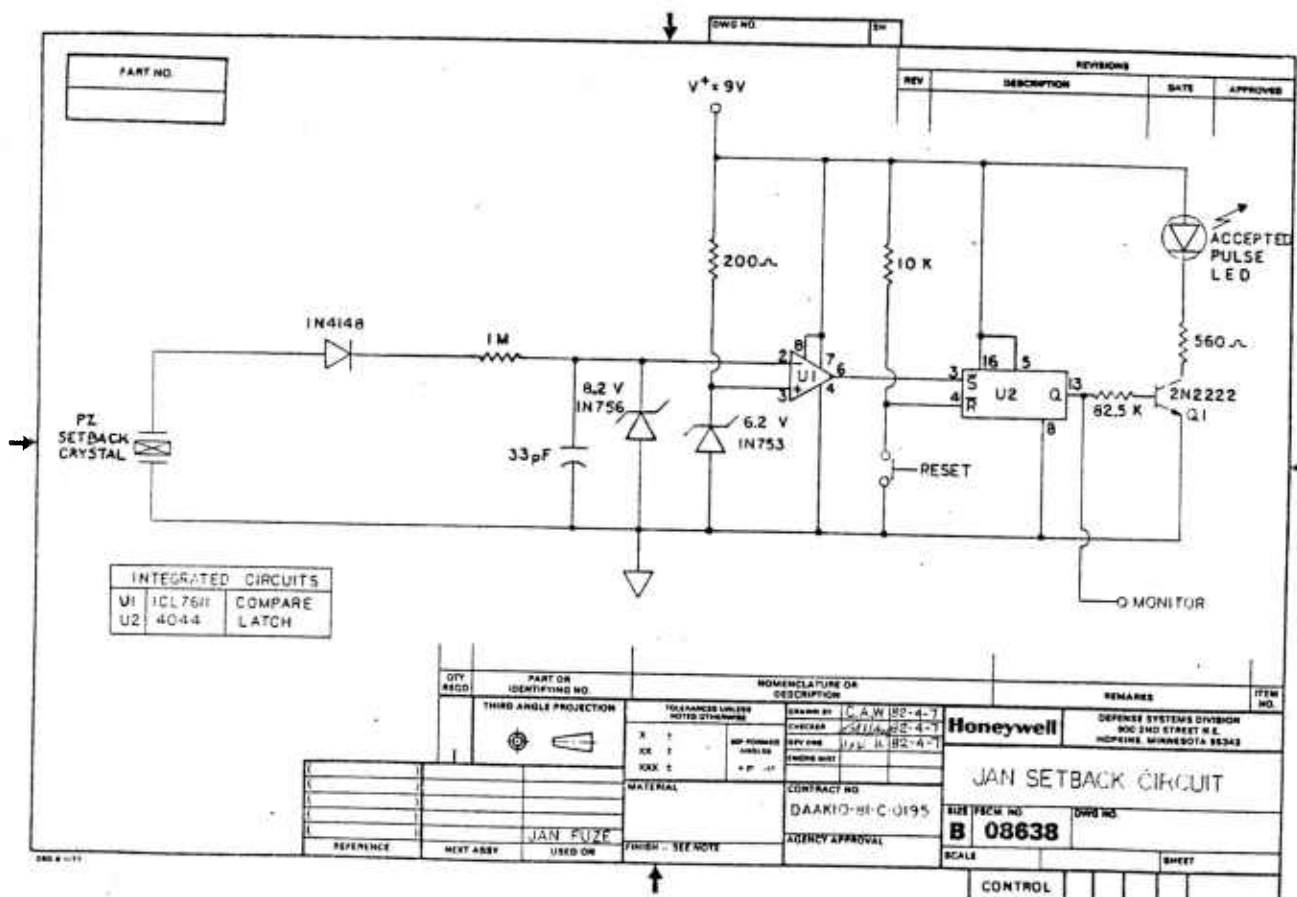


Figure 2-4 Integrated Setback Sensor Circuit

Table 2-2  
Prestress Test Data

<u>Applied Torque</u>	<u>Peak G's</u>	<u>Time to Peak</u>	<u>Set Time</u>
0 in-lbs	733	1.80 msec.	1.24 msec.
2 in-lbs	700	1.72 msec.	1.23 msec.
4 in-lbs	724	1.69 msec.	0.43 msec.
6 in-lbs	754	1.55 msec.	0.29 msec.
8 in-lbs	714	1.64 msec.	0.33 msec.

Engineers connected the setback sensor to an integrator, threshold detector, and display circuit as shown in Figure 2-4. The load capacitor was not required since the piezoelectric crystal output was in a sufficient range without further loading. The 33 pF capacitor and the capacitance of the clipping diode summed to a value sufficient for proper integration. (The HP-41C calculator programs were of limited use due to the unpredictable capacitance of the clipping diode.) We used a 6.2V reference level for the circuit turn on threshold and selected a 4-5 msecond pulse duration to represent typical setback because no pulse duration was specified.

The integrated setback sensor circuit was tested and the data in Figures 2-5 to 2-8 show proper circuit operation. The graphs show the discriminator rejected 440 and 466 G pulses (Figures 2-5 and 2-6), but accepted 575 and 639 G pulses (Figures 2-7 and 2-8). The circuit set on the peak of the 575 G pulse and slightly before the peak of the 639 G pulse. This data demonstrates the circuit will reject a pulse less than 466 G's and will accept a pulse greater than 575 G's so the integrated setback sensor has demonstrated compliance to the 400 G no arm and 600 G all arm requirements.



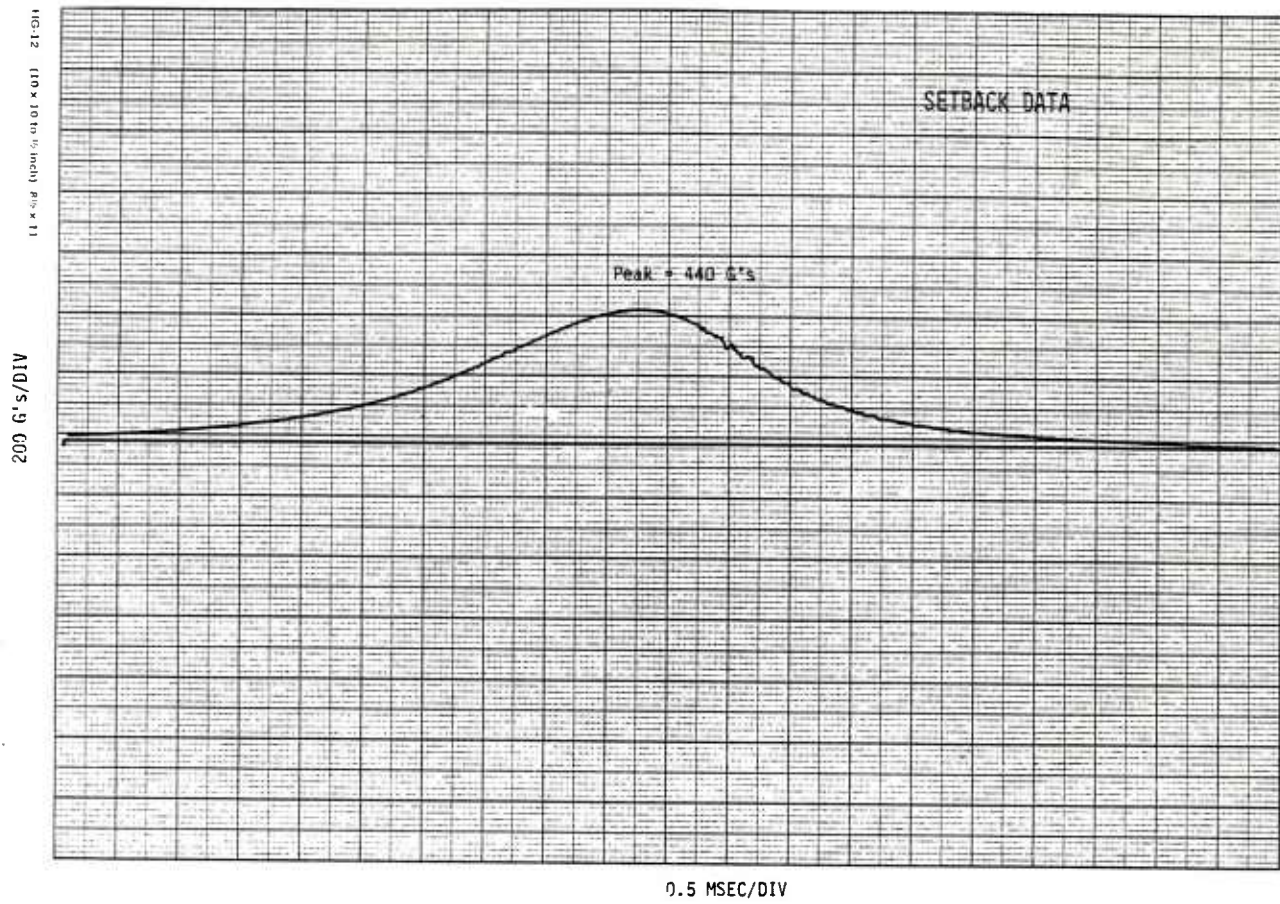


FIGURE 2-5. 440 G SETBACK DATA

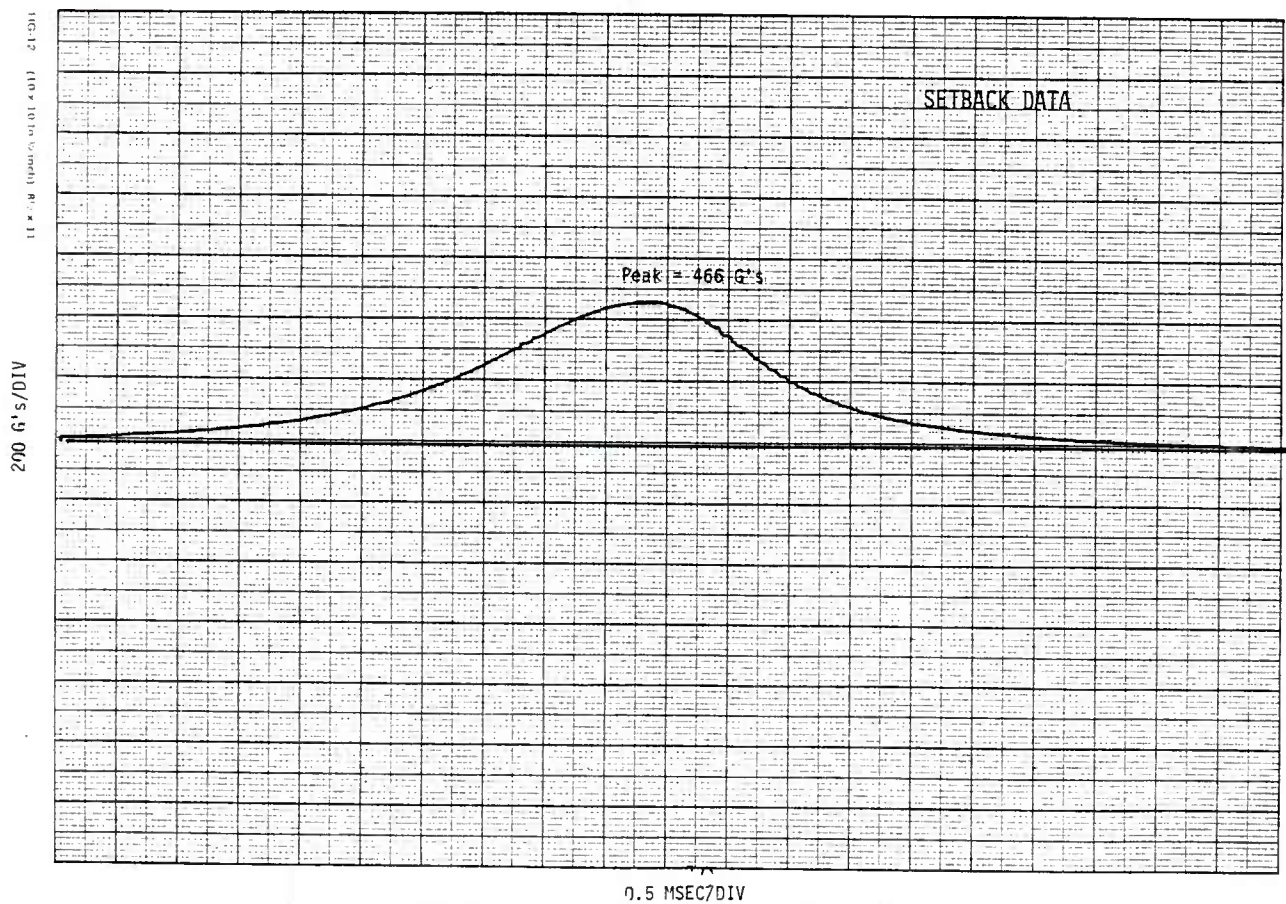


FIGURE 2-6. 466 G SETBACK DATA



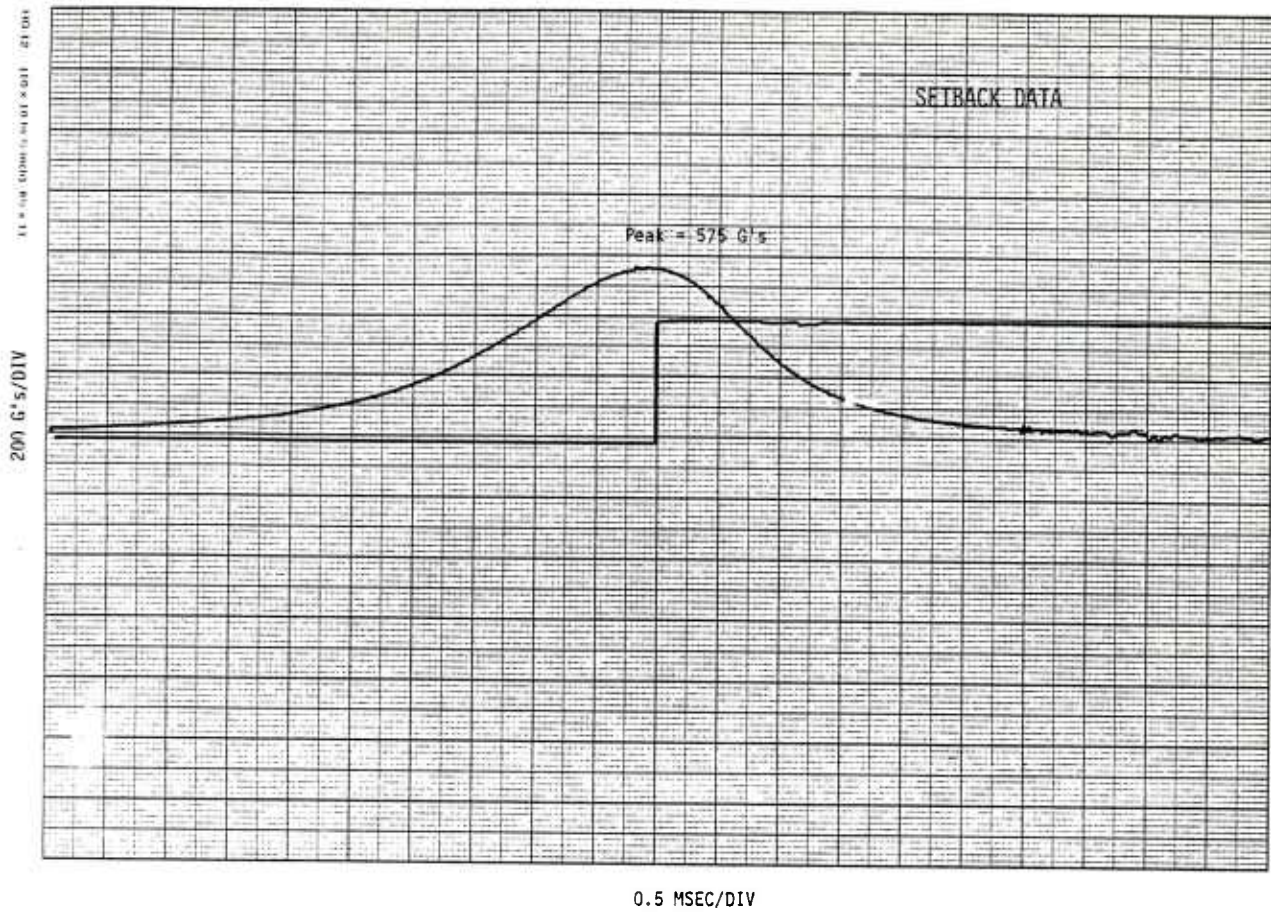


FIGURE 2-7. 575 G SETBACK DATA

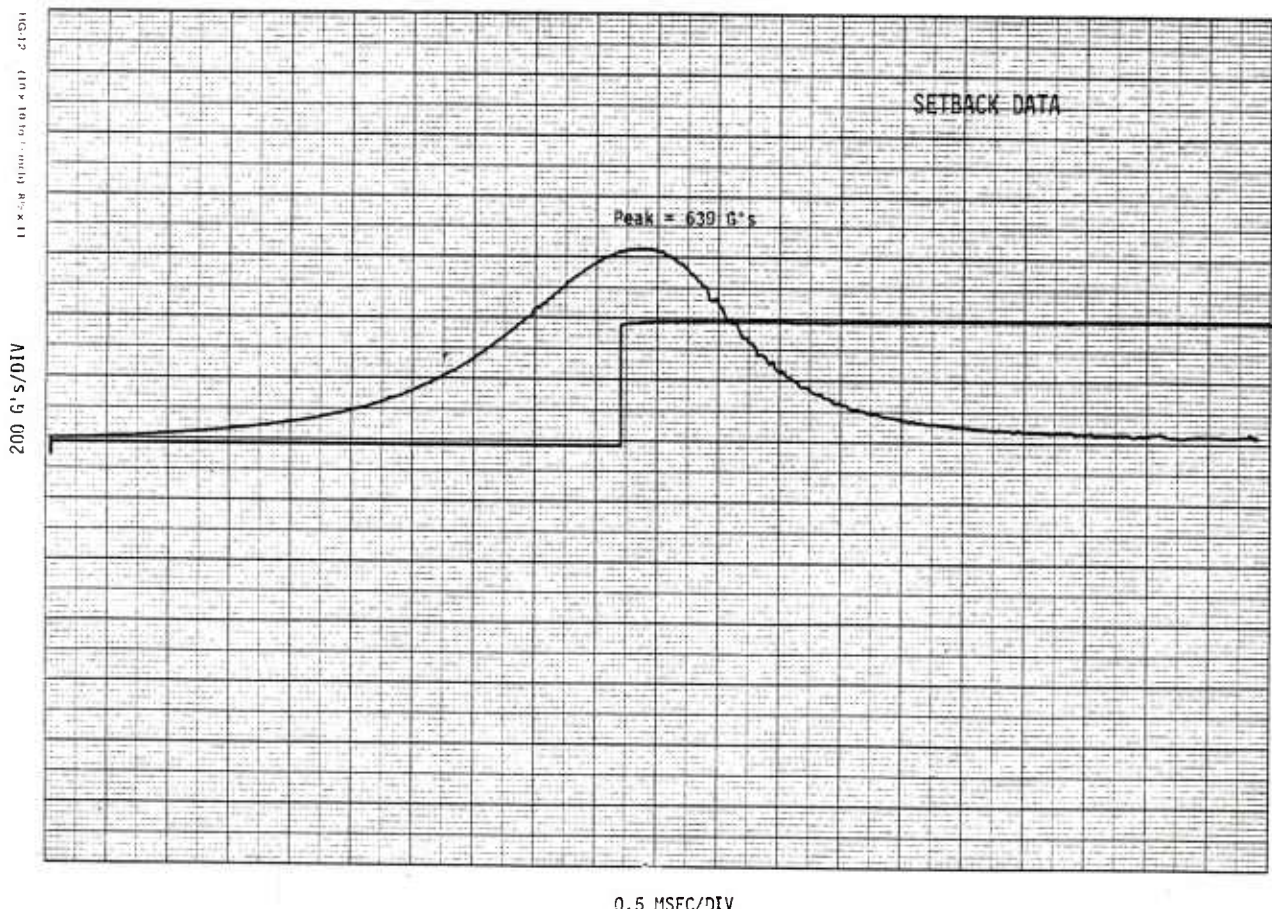


FIGURE 2-8. 639 G SETBACK DATA



The integrated setback sensor circuit was also tested to forty foot type drop conditions. The forty foot drop was simulated by subjecting the integrated setback sensor to a 2000 G, 0.5 msecond (zero to peak) pulse. The integrated setback sensor did accept the pulse as valid, but this result does not imply the fuze would fail a forty foot drop test because the 0.5 msecond (zero to peak) pulse may not be typical of a drop test. Also, the fuze will only arm when the environmental setback supply is initiated, when the proper 1700 RPM spin rate is detected, and when the proper number of revolutions has been counted. The spin rate and number of revolutions environments would probably not be encountered in a forty foot drop test so the integrated setback sensor acceptance of the simulated forty foot drop pulse is not a concern at this time. We conducted the test for completeness of data.

### 3. Revolution Sensor

A revolution sensor is an electronic system which senses and amplifies the earth's magnetic field polarity reversal caused by the revolving of a projectile in flight. The revolution sensor outputs a signal with a frequency proportional to spin rate and this output can be used to determine projectile safe separation distance or projectile spin rate. Projectile safe separation distance can be determined by counting the projectile revolutions because the distance of travel per revolution is known, so counting revolution's relates to a fixed distance of travel. Projectile spin rate can be classified as all-arm or no-arm by comparing the frequency output of the revolution sensor to a standard time base. A frequency higher than the standard indicates a proper spin rate so the fuze is in the all-arm spin rate mode, while a frequency lower than the standard indicates low spin rate and puts the fuze in the no-arm mode.

Several types of magnetic sensors are available which can sufficiently detect the earth's magnetic polarity reversal associated with projectile spin. The ideal requirements for a JAN fuze revolution sensor are:

- o Sense spin rates from 1000 to 30,000 revolutions per minute
- o Spin sensitivity regardless of flight direction
- o Low power
- o Low cost
- o Small size
- o Suitable for high volume production

The magnetic sensors studied to date include: air core sense coils, magneto-resistive bridge magnetometers, pole piece magnetometers, and magnetometers currently used in high volume mine production programs. We constructed a versatile spin fixture for evaluation of the JAN revolution sensor candidates.

### 3.1 Spin Fixture

The spin fixture was constructed to enable spinning of sensor candidates at various spin rates and directions. A precise motor speed control was used to regulate the motor C.W. or C.C.W. direction spin rate from 0 to 3000 rpm. The motor was mounted to an aluminum section which could be adjusted and held to various angles above horizontal. The sensor candidates were placed in an ogive which connected to the motor via a four foot aluminum shaft, used to minimize motor to sensor interference. A cavity below the ogive contained the revolution sensor amplifier and electrical connection from the amplifier to the monitoring equipment was made via three carbon brush contacts. Testing in any compass

direction could easily be conducted because the entire spin fixture assembly was mounted to a portable cart.

A photograph of the fixture and motor speed control unit is shown in Figure 3-1. The photograph was taken in front of storage cabinets so the vertical lines shown are cabinet door edges and not part of the spin fixture. The motor speed control is in the lower portion of the picture and the motor is on the right. The ogive and electronic cavity are shown at the end of the aluminum shaft just after the brush contact assembly at the upper left. The shaft on the left third of the picture which is tilted slightly to the right is a threaded shaft, used to hold the ogive and motor assembly at a particular angle during testing. The angle above horizontal adjusts by raising or lowering the support nuts on the threaded support shaft.

The spin fixture was used extensively for sensor evaluation. Sensor candidates were evaluated by determining how close the sensor spin axis could be to an orientation parallel to the earth's lines of flux for revolution detection. The sensitivity window was defined as that region where a non-saturating amplifier output was observed and was recorded for each sensor test. We found that this procedure was most accurate since the data reveals true sensitivity and not merely relative performance determined by comparing one candidate to another. For testing conducted at the Honeywell facility in Hopkins, Mn., we collected the sensitivity data with the spin fixture pointing parallel to the incoming lines of flux, approximately south at  $70^{\circ}$ . The sensitivity window was determined by recording the angles which produced no sensor output so the sensor performance could be accurately determined and reported. The method was used for all sensor evaluations.



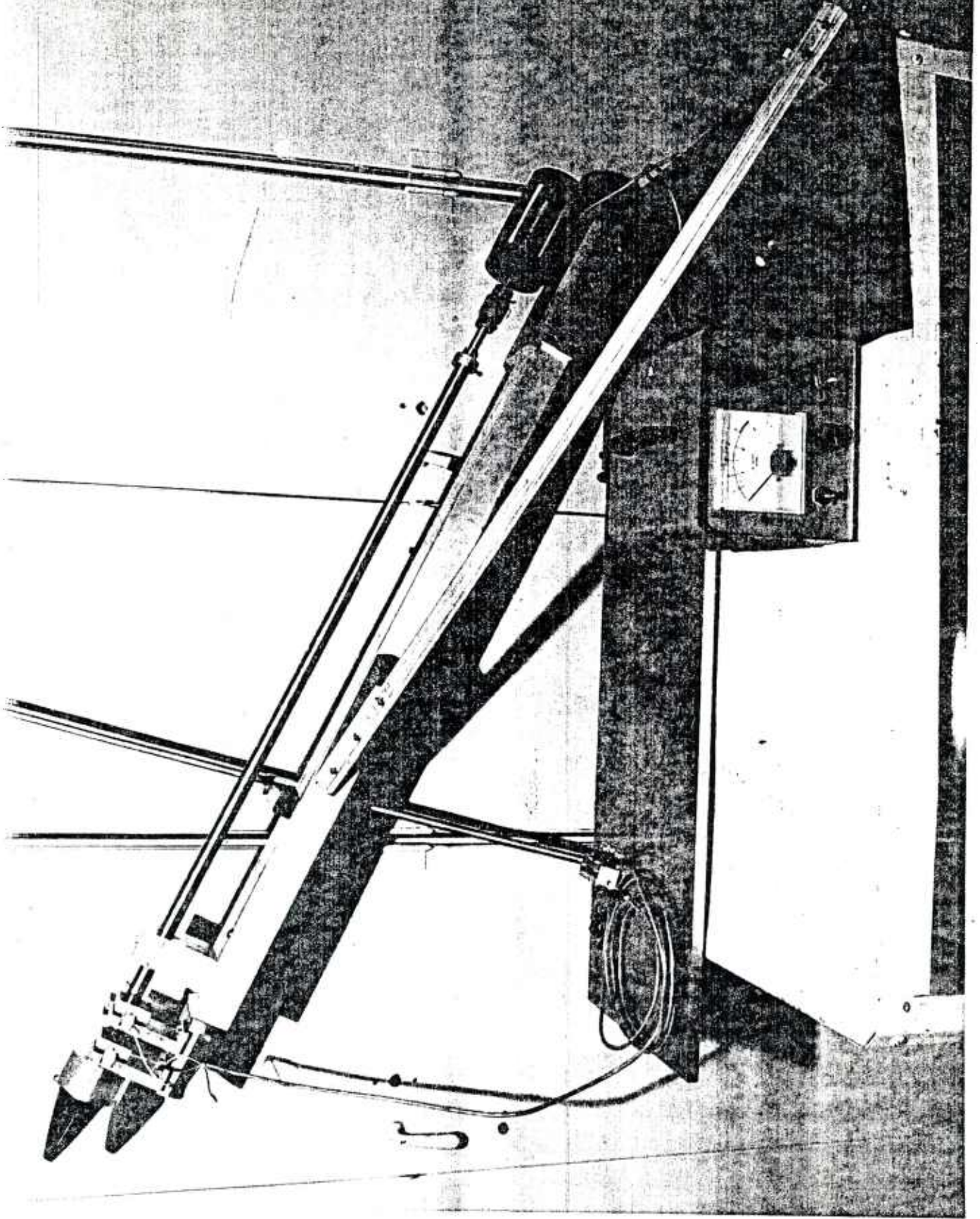


FIGURE 3-1. JAN SPIN FIXTURE

### 3.2 First Program Development

Honeywell evaluated three revolution sensor candidates in the first JAN fuze initial exploratory development program (contract DAAK10-80-C-0049), completed in October of 1980. During the first program, some air core sense coils were obtained from a previously conducted Honeywell Internal Development program and designated as "old coils." Two old coils were connected in series to make a revolution sensor and each coil was constructed with 250 turns of #26 wire wound in a 2 1/2" x 1" oval shape. Two "new coils" were constructed in the first program and also connected in series to make a revolution sensor. Each new coil was built with 1000 turns of #44 wire wound in a "horse collar" shape approximately 2" high with a 1 1/2" base. The third revolution sensor evaluated in the first effort program was a magnetoresistive bridge magnetometer, or MRB. The MRB sensor is an integrated magnetometer consisting of four Nickel-Iron (NiFe) thin film magnetoresistors connected in a bridge configuration. Each magnetoresistive element is biased and changes resistance when an external magnetic field is detected resulting in a resultant MRB output signal proportional to the magnetic field encountered. The major advantage of this device is its small size and process compatibility with integrated circuit technology which would enable the MRB and amplifier to be fabricated on one integrated circuit. This results in a high volume and low cost potential inherent with large scale integrated circuits.

In the first program, engineers tested the old coils, new coils, and MRB devices to determine sensor output as a function of spin rate. The sensors were connected to a 55 db spin rate amplifier, Figure 3-2, operated from a 10 volt supply and testing was conducted with the spin fixture pointing south at 30° and

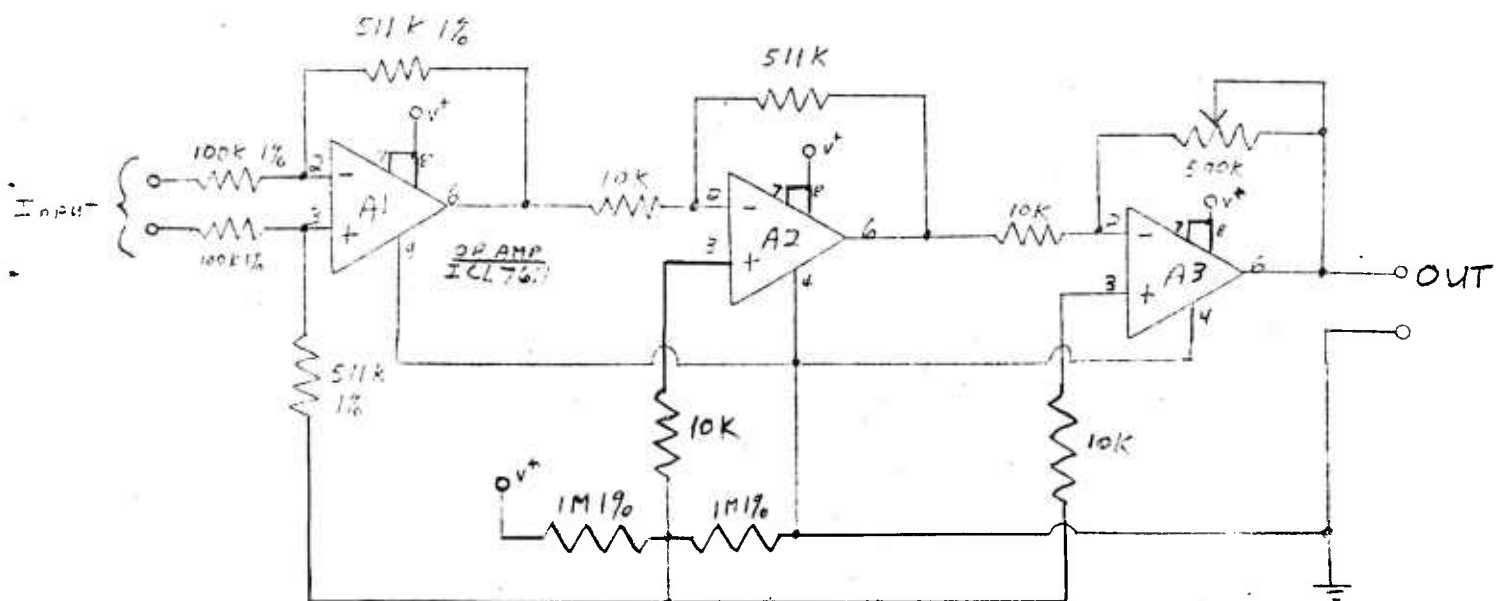
TABLE 3-1

REVOLUTION SENSOR OUTPUT V.S. SPIN RATE (RPM)

RPM	MRB	South at 30°		MRB	West at 0°	
		Old Coils	New Coils		Old Coils	New Coils
200	0.5	0.2	0.2	0.6	0.3	0.2
400	1.0	1.0	0.6	1.2	1.3	0.7
600	1.5	2.2	1.2	1.8	2.7	1.7
800	2.0	4.0	2.3	2.4	4.6	3.6
1000	2.5	6.0	3.5	3.0	7.5	4.5
1200	3.0	8.5	5.0	3.6	10.0	7.0
1400	3.5	10.0	7.2	4.2	10.0	9.0
1600	4.0	10.0	9.5	5.0	10.0	10.0
1800	4.5	10.0	10.0	5.5	10.0	10.0
2000	5.0	10.0	10.0	6.0	10.0	10.0

 $(V_{in} = 10.0 \text{ Volts})$ 

FIGURE 3-2. SPIN RATE AMPLIFIER



pointing west at  $0^0$ . The data is presented in Table 3-1 and shows the MRB is slightly more spin rate sensitive than the new coils. We determined that the data revealed no significant performance variances so sensitivity window testing was conducted.

The first program sensitivity window tests were conducted with the amplifier gain increased, so easy saturation was possible. The tests were conducted for decreasing amplifier input voltages because the JAN fuze supply voltage is expected to decrease during flight. The sensitivity window was determined and recorded for all candidates. Those results are presented in Table 3-2 and the amplifier circuit used is presented in Figure 3-3.

The MRB was not as sensitive as either coils. This fact, in addition to the required bias current (150 uA), caused us to drop the MRB from contention as the revolution sensor. The new coils had better performance than the old coils at low amplifier input voltage levels which, in addition to the larger size of the old coils, caused them to also be rejected as the JAN revolution sensor. This conclusion ended the revolution sensor development of the initial exploratory development program, but revolution sensor development continued in the continued exploratory development program described by this report.

### 3.3 Second Program Development

Engineers studied three types of revolution sensors in this continued exploratory development program: air core sense coils, pole piece magnetometers, and RAAM (Remote Artillery Antiarmor Mine) magnetometers. We investigated the sensitivity effects of mounting orientation, spin fixture

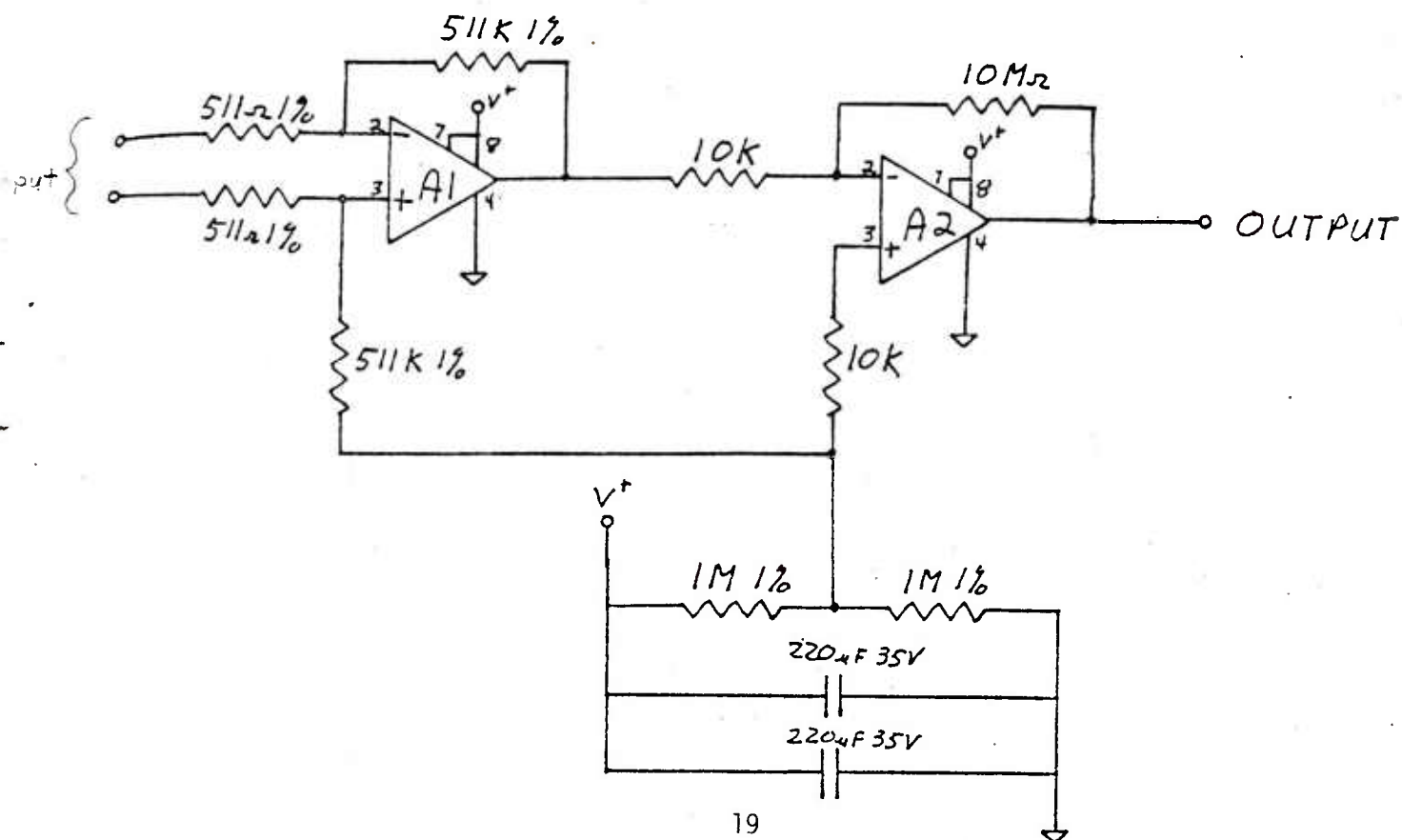


TABLE 3-2. FIRST PROGRAM SENSITIVITY WINDOW DATA

<u>VOLTAGE IN</u>	<u>M.R.B. WINDOW</u>	<u>OLD COIL WINDOW</u>	<u>NEW COIL WINDOW</u>
10.0	67° - 72°	69° - 71°	69° - 71°
9.5	67° - 72°	69° - 71°	69° - 71°
9.0	67° - 72°	69° - 71°	69° - 71°
8.5	67° - 72°	69° - 71°	69° - 71°
8.0	67° - 72°	69° - 71°	69° - 71°
7.5	67° - 72°	69° - 71°	69° - 71°
7.0	67° - 72°	69° - 71°	69° - 71°
6.5	67° - 72°	68° - 72°	69° - 71°
6.0	67° - 72°	67° - 73°	68° - 72°
5.5	67° - 72°	66° - 75°	68° - 72°
5.0	66° - 73°	64° - 76°	67° - 73°
4.5	66° - 73°	63° - 77°	67° - 73°
4.0	66° - 73°	63° - 77°	67° - 73°

NOTE: All tests done with fixture pointing south  
spin rate = 1000 rpm

FIGURE 3-3. REVOLUTION SENSOR AMPLIFIER





aluminum ogive presence, penetrator presence, and sensor construction. The development and evaluation of many sensor candidates resulted in the definition of a JAN fuze revolution sensor which is small, sensitive, and easily adaptable to current high volume production technology.

One type of revolution sensor candidate which was unsuccessfully tested was the low cost RAAM magnetometer currently being volume produced by Honeywell for the FASCAM program. The magnetometer consists of a torriod core wound with wire which is encapsulated in a small plastic package. In the normal mode of operation, the magnetometer is pulsed by an oscillator and driver circuit and a magnetic anomaly output is generated after rectifying and filtering. The JAN fuze does not have power available to operate the RAAM magnetometer in the active mode, so we conducted testing to determine if this high volume, low cost device would sufficiently operate in a passive mode as a revolution sensor. The program engineers spin fixture tested single and dual magnetometers in many mounting orientations to evaluate performance. The magnetometers were connected to the amplifier in Figure 3-3 and spun at 1000 rpm, but no output was detected unless a magnet or screwdriver was brought within a few inches of the device under test. We therefore rejected the RAAM magnetometer as a JAN fuze revolution sensor candidate.

Engineers found acceptable results when they conducted single and dual air core sense coil tests. The single v.s. dual tests were done with 500 turns of #37 wire coils and indicated the dual system sensitivity was much better than the single system sensitivity. Testing was conducted with and without the aluminum ogive for the 500 turns of #37 wire dual coil setup. The results indicated a minor sensitivity difference due to the ogive presence. A dual coil 1000 turns of #44

wire system was compared to a dual 500 turns of #37 wire system and the results indicated the 1000 turns of #44 wire coils performed slightly better than the 500 turns of #37 wire coils. A data summary is presented in Table 3-3 and the table shows it is possible to get revolution window sensitivity of  $\pm 1^0$  when using the air core sense coils.

The testing was conducted with the coils mounted on a wooden holder which was attached to the spin fixture. Engineers wanted to determine what effect the fuze penetrator would have on coil revolution sensing performance so a 739 penetrator (made from 1144 steel) was obtained and mounted to the spin fixture. We conducted three performance tests with two 500 turn #37 wire coils, where the coil position relative to the penetrator was varied. The coils were mounted towards the penetrator base for test 1, half way up the penetrator for test 2, and towards the top for test 3 as shown by Figure 3-4. The penetrator sensitivity window test data, Table 3-4, shows negligible differences due to relative coil position. The penetrator v.s. nonpenetrator present data shows slightly increased sensitivity due to the presence of the penetrator so the penetrator attracts flux lines, thereby improving coil performance.

The final type of revolution sensor candidate studied was a pole piece magnetometer constructed by winding wire onto a ferrous core. The sensitivity of the pole piece is governed by the length over diameter ratio, number of turns of wire, and pole face area. Honeywell engineers constructed a pole piece magnetometer from a 7/16" diameter steel rod cut to a 1" length. The rod was machined to a "hourglass" shape to enable winding of more wire and the pole piece was mounted orthogonal to the spin axis on the spin fixture. The two leads of the pole piece were connected to the input of the revolution amplifier previously

TABLE 3-3  
COIL SENSITIVITY WINDOW V.S.  
AMPLIFIER INPUT VOLTAGE

Vin	Test 1 Window	Test 2 Window	Test 3 Window	Test 4 Window
4.0	69.5 - 72.5	67 - 77	68 - 72	68 - 72
4.5	70 - 72	↓	↓	↓
5.0	↓	67.5 - 76.5	↓	69 - 72
5.5	↓	↓	↓	↓
6.0	↓	67.5 - 76	↓	↓
6.5	↓	↓	↓	↓
7.0	↓	68 - 76	↓	70 - 72
7.5	↓	↓	↓	↓
8.0	↓	↓	↓	↓
8.5	↓	↓	↓	↓
9.0	↓	68.5 - 75.5	69 - 71	↓
9.5	↓	69 - 75	↓	↓

- Notes:
- 1) All voltages are in volts
  - 2) Spin rate = 1000 rpm
  - 3) Sensitivity window is in degrees
  - 4) Test 1: 2 coils, 1000 turns #44 wire each, with ogive
  - 5) Test 2: 1 coil, 500 turns #37 wire, without ogive
  - 6) Test 3: 2 coils, 500 turns #37 wire each, with ogive
  - 7) Test 4: 2 coils, 500 turns #37 wire each, without ogive

FIGURE 3-4. PENETRATOR TEST ORIENTATION

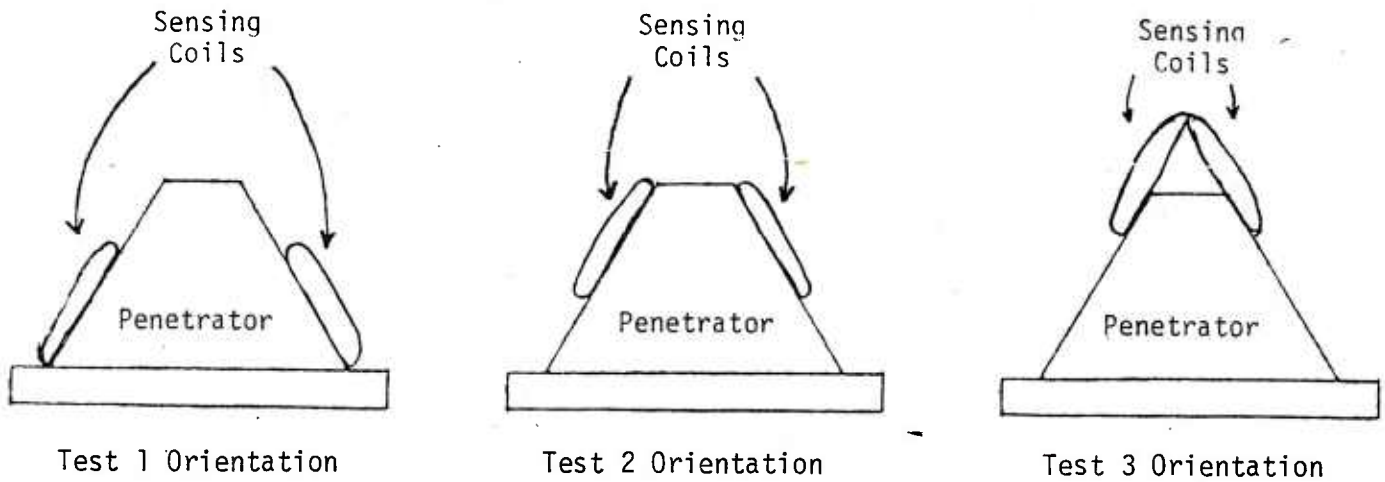


TABLE 3-4.

COIL PENETRATOR V.S. NON PENETRATOR SENSITIVITY DATA

Vin	Test 1 Window	Test 2 Window	Test 3 Window	No-Penetrator Window
4.0	70-72.5	69.5-72.5	69.5-72.5	68-72
5.0	70-72.5	69.5-72.5	69.5-72.5	69-72
6.0	70-72.5	70-72.5	70-72	69-72
7.0	70-72	70-72	70-72	70-72
8.0	70-72	70-72	70-72	70-72
9.0	70-72	70-72	70-72	70-72
10.0	70-72	70-72	70-72	70-72

NOTE: Sensitivity window is in degrees, input voltage is in volts, and spin rate was 1000 rpm.

used and tested with the pole piece mounted above the penetrator described in previous testing. The spin fixture ran at 1000 rpm while pointing south and the sensitivity windows for various pole pieces were recorded.

The first hourglass pole piece tested was constructed with 1000 turns of #37 wire. The sensitivity of this device was  $\pm 5^\circ$  at an amplifier voltage of 4.0 volts and  $\pm 3^\circ$  at 10.0 volts. A second pole piece was built from 2000 turns of #37 wire and the sensitivity of this device ranged from approximately  $\pm 3^\circ$  to  $\pm 1.5^\circ$ . The 2000 turns of #37 wire filled the pole piece core so a third pole piece was constructed from 2000 turns of smaller #44 wire. This device had a sensitivity range of approximately  $\pm 3^\circ$  to  $\pm 1.5^\circ$  and had room for additional wire, so a fourth pole piece was constructed. The pole piece core was wound with #44 wire until it was filled to a near cylindric shape, which occurred at 6000 turns. We determined that this device performed slightly better than the best air core sensing coils, which were constructed from 1000 turns of #44 wire each.

We attempted to reduce the pole piece mass by using a "dumbbell" shaped core. Several dumbbell pole piece cores were machined from a 7/16" diameter steel rod. The 1" long cores, wound with 6000 turns of #44 wire, were tested with the same setup as the 6000 turns of #44 wire hourglass pole pieces. The pole piece sensitivity data is presented in Table 3-5. As shown by the test data, the dumbbell shaped pole piece does not perform as well as the hourglass pole piece. Improved dumbbell pole piece performance could be obtained by winding additional wire onto the core, but the density of wire is greater than the density of the steel rod so additional wire would increase pole piece weight. Therefore, the best performance to weight ratio is obtained by using the hourglass configuration.

TABLE 3-5  
POLE PIECE SENSITIVITY WINDOW DATA

Amplifier Voltage	Hourglass Pole Piece Data			
Vin	1000 T #37 Wire	2000 T #37 Wire	2000 T #44 Wire	6000 T #44 Wire
4.0	66-76	68.5-74	69-74	69.5-72
5.0	66.5-75.5	68.5-74	69.5-74	69.5-72
6.0	67-75.5	69-74	70-74	70-72
7.0	67.5-75	69-74	70-73.5	70-72
8.0	67.5-75	69-73.5	70-73.5	70-72
9.0	67.5-74	70-73	70-73.5	70-71.5
10.0	68-74	70-73	70-73	70-71.5

Amplifier Voltage	Barbell Shape Pole Piece 6000T, #44 Wire	Best Air Coils, 1000 T #44 Wire Ea.
Vin		
4.0	69.5 - 73.5	69.5 - 72.5
5.0	70.0 - 73.5	70 - 72
6.0	70.0 - 73.5	70 - 72
7.0	70.5 - 73.5	70 - 72
8.0	70.5 - 73.0	70 - 72
9.0	70.5 - 73.0	70 - 72
10.0	70.5 - 72.5	70 - 72

NOTE: Sensitivity window is in degrees, input voltage is in volts, spin rate was 1000 rpm, and pole pieces were mounted on the penetrator.

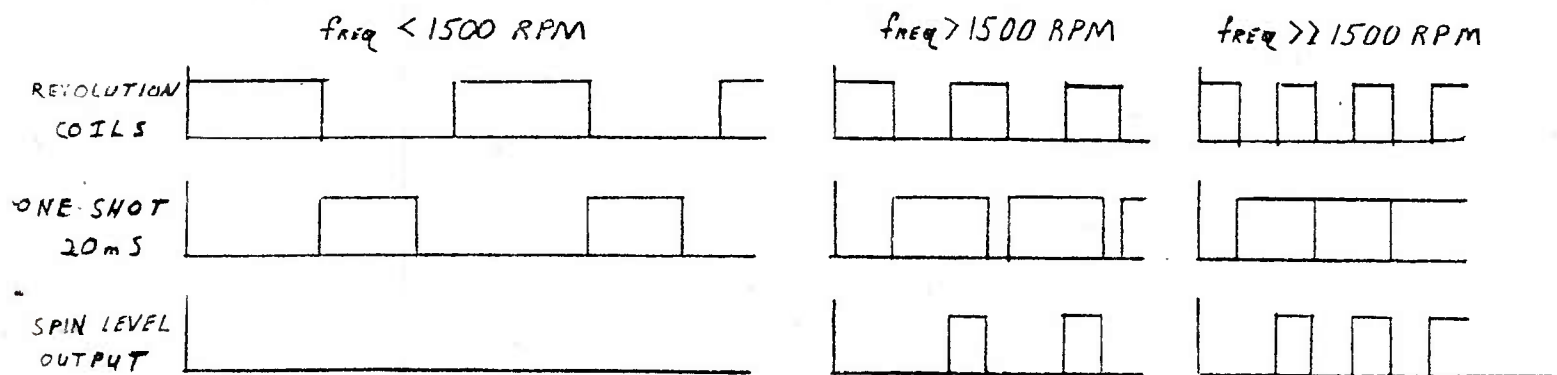
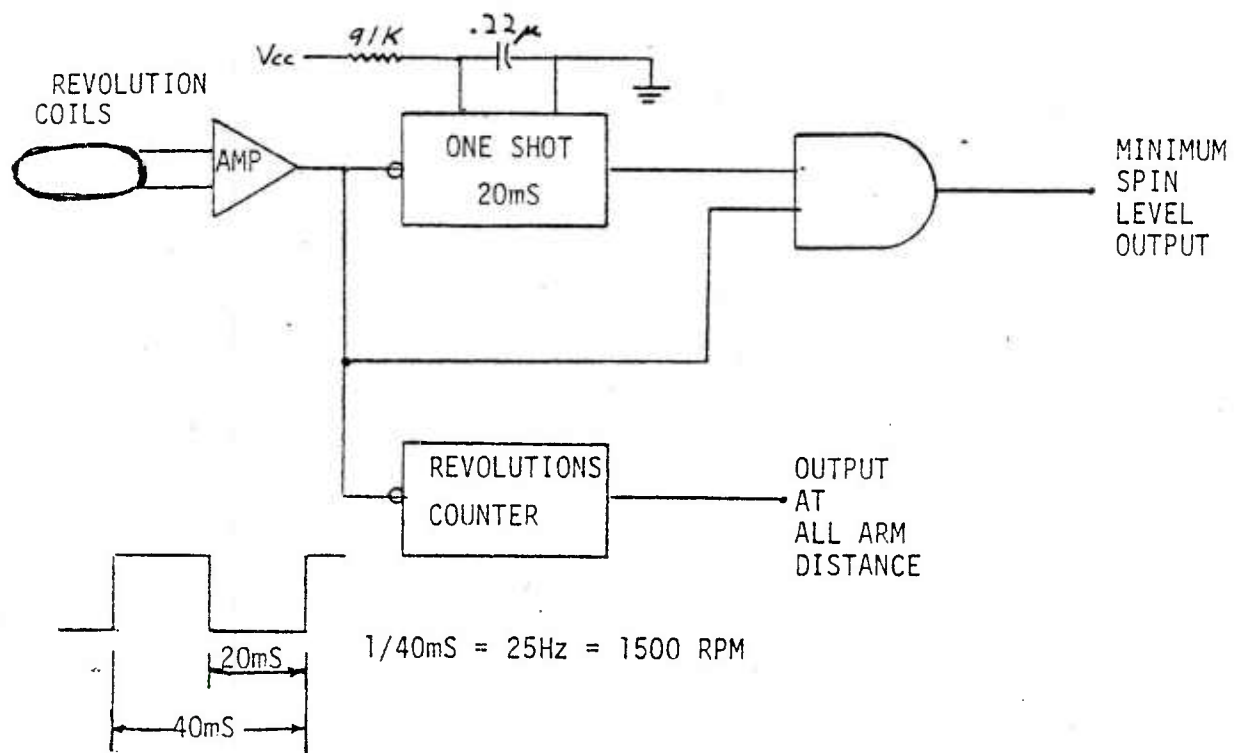
The development of a hourglass core pole piece which can perform slightly better than air core coils is significant because this device is a low cost alternate to the air core sensing coil. At high production levels, programmed lathes would automatically machine the steel core to the proper shape, automatic coil winders would apply the proper number of wire turns, and the device would be encapsulated in a small package with solder lugs for easy component connection. Fuze construction using the small encapsulated pole piece assembly would be much easier than using two large sensing coils, so the pole piece feasibility demonstration was an exciting breakthrough from a cost, production, and assembly standpoint. We have therefore selected the pole piece magnetometer as the primary JAN fuze revolution sensor.

#### 4. Spin Rate Detector

Fuze spin rate is electrically monitored and used as the second environment in the JAN fuze arming sequence. The revolution sensor outputs a signal proportional to spin rate which is compared to a time base standard to evaluate the fuze spin rate. A proper spin rate satisfies the second of three criteria necessary for fuze arming.

We demonstrated the feasibility of discerning spin rate in the first JAN program and the circuit used is shown in Figure 4-1. The revolution sensor amplifier outputs a square wave with a frequency proportional to fuze spin rate. We selected a detection threshold of 1500 rpm because the Army spin rate requirement is no arm at 1100 rpm and all arm at 1700 rpm. The revolution sensor output will trigger the one shot and the one shot timeout is compared with the revolution sensor output by an AND gate. If the spin rate is less than 1500 rpm, the one

FIGURE 4-1. SPIN RATE DETECTOR





shot output will be L0 before the next revolution sensor input goes HI, resulting in the output of the AND gate always being L0. If the spin rate is above 1500 rpm, the output of the one shot will still be HI when the next revolution sensor input goes HI, resulting in a HI output from the AND gate which indicates the minimum spin rate threshold has been achieved.

In the first year program, engineers tested the spin rate detector circuit with sense coils, but the circuit will operate as well when used with a pole piece sensor. We built the spin rate detector circuit into the demonstrator model using a pole piece sensor and excellent results were observed. That circuit is presented and discussed in the demonstrator section of this report.

## 5. Revolution Counter

The revolution counter is used to discern safe separation distance by using the output of the revolution amplifier to increment a digital counter which counts fuze revolutions. Safe separation distance has occurred when the revolution counter has counted a specified number of revolutions. The revolution counter outputs a signal to the fuze electronics to indicate compliance to the third arm environment causing the electronics to put the detonator in line which arms the fuze. The fuze will now detonate upon impact.

Program personnel have successfully demonstrated the revolution counter concept and therefore included it in the JAN fuze demonstrator. We designed the demonstrator to count 32 revolutions and a description of the demonstrator unit is presented in subsequent sections of this report.

## 6. Programmable Feasibility

The Department of Defense uses programmable Multi-Option fuzes to achieve increased weapon effectiveness. A Setter Control Unit (SCU) is used to program a fuze prior to launch by magnetically transferring information to the fuze which then retransmits the information to the SCU for verification. The Navy constructs the EX416 and EX419 multi-option fuzes with a bobbin coil used as a magnetic receiver link to enable information transfer between the SCU and fuze. The Navy expressed interest in using the JAN revolution sensor as a magnetic receiver link, so testing was conducted to determine the feasibility of using the revolution sensor to program the JAN fuze.

Alan Wendler of Honeywell and Chuck Johnson of the Naval Surface Weapons Center conducted magnetic energy and intelligence transfer tests in February of 1982. They conducted testing at NSWC which included recording the induced voltage from the SCU when a revolution sensor candidate was connected to a 10K load resistor. They also recorded the induced fuze logic voltage when the sensor candidate was connected to an EX416 fuze. Air core sense coils, pole pieces, and RAAM magnetometers were tested and the results compared to the performance of the standard EX416 receiver link. This comparison revealed that none of the tested JAN revolution sensor candidates had acceptable performance as a receiver coil link when used with the current Setter Control Unit, but modifications to the SCU or JAN sensors may result in acceptable future performance.

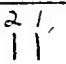
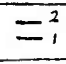
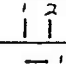
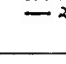
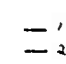
Engineers collected data at various sensor orientations since the magnetic field produced by the Setter Control Unit is not symmetrical due to the tear drop shape of the transmitting coil. Two sense coils were mounted on a wooden coil holder

which was attached to a wooden rod and suspended near the SCU transmitting coil. Two 500 turns #37 wire coils were tested and two 1000 turns #44 wire coils were tested. The data for the 500 turns, #37 wire coils is shown in Table 6-1 and the data for the 1000 turns, #44 wire coils is shown in Table 6-2. The induced voltages (with  $R_L = 10K$ ) on each coil are given for each orientation and also the output voltages when the coils were connected in the various parallel and series test configurations are presented. We found the sense coil revolution sensors to be sometimes directional and overall not as sensitive as the standard EX416 receiver coil.

We wanted to test all sensor candidates so a 6000 turns, #44 wire hourglass pole piece was mounted vertical to the transmitting coil and tested. We found only 0.44V was induced on the 10K load resistor and only 1.1V was induced in the EX416 fuze when the device was directly connected to the EX416 fuze.

The 2000 turns, #44 wire hourglass pole piece was damaged in transit so no data was collected, but performance only slightly better than the 6000 turns, #44 wire pole piece was expected due to lower device resistance. The 6000 turns, #44 wire dumbbell pole piece had 1.8V at a horizontal orientation and 2.2V at a vertical orientation, but no logic voltage was detected when it was connected to the fuze. A RAAM magnetometer achieved a maximum load resistor voltage of 4V when mounted parallel to the transmitting coil face, but no logic voltage was detected when this device was connected to the EX416 fuze. These results show that performance with the tested hardware is not acceptable and further effort is needed to develop this concept.

Table 6-1  
Voltage Transfer Data  
500T #37 Coils

Orientation	V <sub>1</sub>	V <sub>2</sub>	TC1	TC2	TC3	TC4
	8.4	1.5	2.6	2.6	6.2	7.1
	1.5	14	5.2	10.2	7.4	9.0
	7.8	2.9	3.0	6.0	6.5	6.8
	18	7	12	13.8	8.2	8.2
	Logic Voltage		.70	1.36	.79	.4

NOTES: Tuned output (.0038 uF) of EX416 coil on 10K load = 21V. Maximum JAN coil output was obtained with out any tuning capacitor.

V<sub>1</sub> = output of coil 1 only.

V<sub>2</sub> = output of coil 2 only.

TC1 (Test configuration 1)	+coil 1 to -coil 2	Series
TC2	-coil 1 to -coil 2 +coil 1 to +coil 2	Parallel
TC3	+coil 1 to -coil 2 -coil 1 to +coil 2	Parallel
TC4	-coil 1 to -coil 2	Series

Table 6-2

## Voltage Transfer Data

1000T #44 Coils

Orientation	$V_1$	$V_2$	TC1	TC2	TC3	TC4
$\begin{smallmatrix} 2' \\ 11 \end{smallmatrix}$	5.6	1.8	2.5	1.3	0.24	1.3
$\begin{smallmatrix} -2' \\ -11 \end{smallmatrix}$	3.3	5.6	1.7	5.5	0.1	2.0
$\begin{smallmatrix} 1' \\ 11 \end{smallmatrix}$	4.4	2.5	1.8	0.5	0.18	1.7
$\begin{smallmatrix} -1' \\ -11 \end{smallmatrix}$	8.1	0.4	5.1	4.7	0.15	2.8

All Fuze Logic Readings Negligable

NOTES: Tuned output (.0038  $\mu$ F) of EX416 coil on 10K load = 21V. Maximum JAN coil output was obtained with out any tuning capacitor.

$V_1$  = output of coil 1 only.

$V_2$  = output of coil 2 only.

TC1 (Test configuration 1)	+coil 1 to -coil 2	Series
TC2	-coil 1 to -coil 2 +coil 1 to +coil 2	Parallel
TC3	+coil 1 to -coil 2 -coil 1 to +coil 2	Parallel
TC4	-coil 1 to -coil 2	Series

## 7. Impact Sensor

Engineers selected a piezoelectric impact sensor for use in the JAN fuze due to its quick response, small size, and proven performance on the Copperhead and Advanced Lightweight Torpedo programs. The piezoelectric crystal senses shock waves generated at impact and outputs a signal for Super Quick or Auto Delay mode detonation. The Super Quick or Auto Delay mode option is selected by the fuze body selector switch which is monitored by the electronics. Impact in the Super Quick mode results in immediate detonation while impact in the Auto Delay mode results in delayed detonation after the target void is detected.

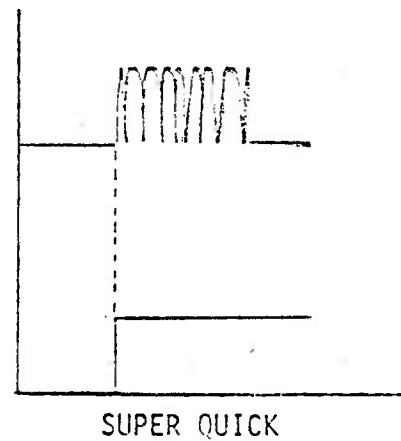
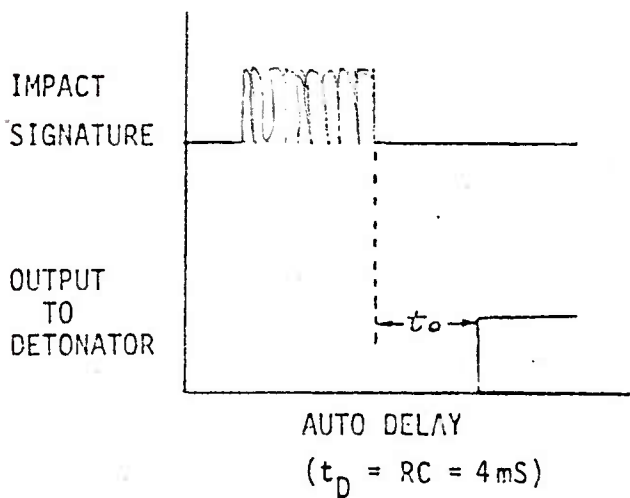
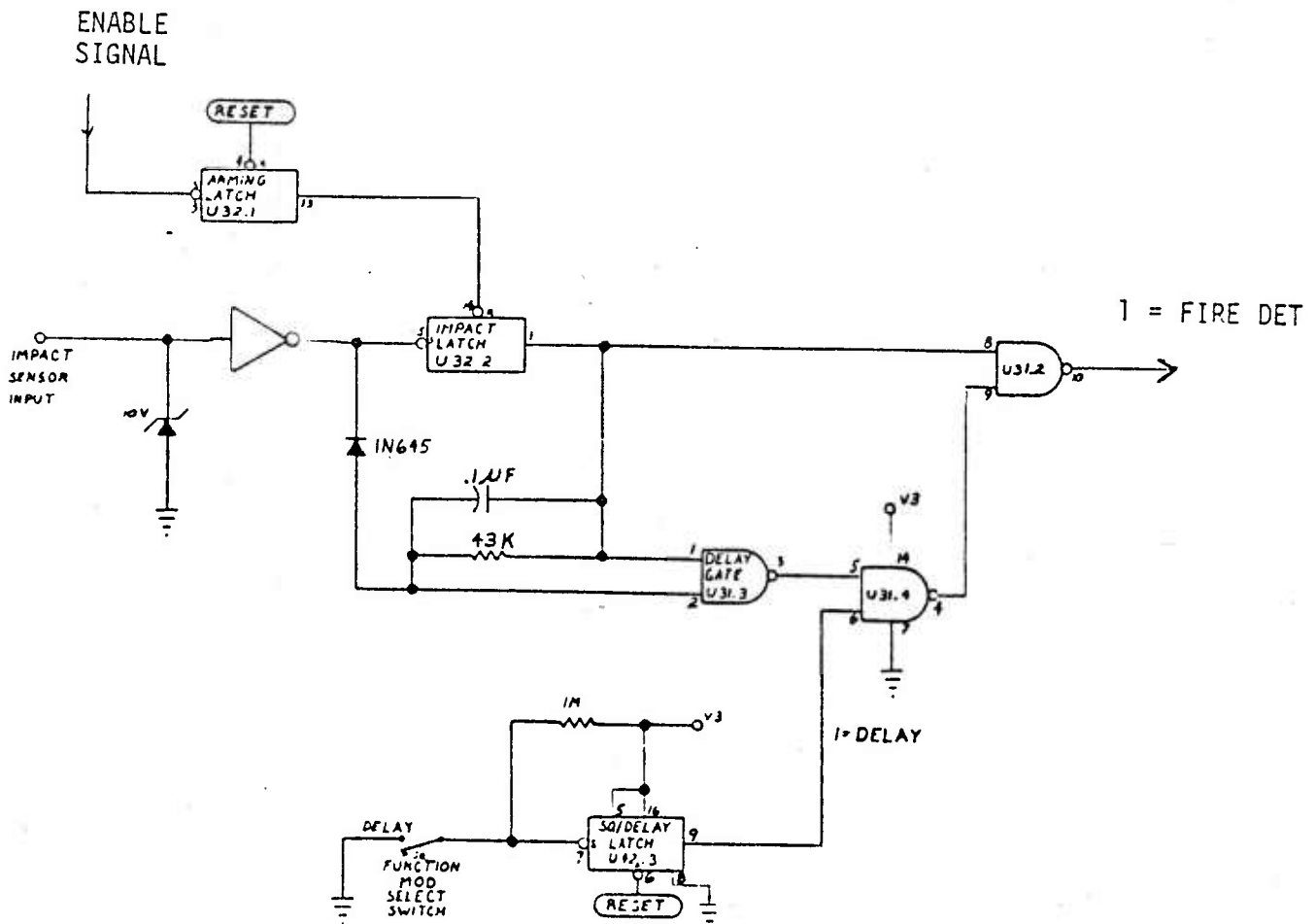
In the Auto Delay mode, the impact circuit envelope detects the pulse modulated waves generated by the impact sensor. The impact Super Quick/Auto Delay circuit, Figure 7-1, is enabled after the revolution counter determines the proper safe separation distance by counting projectile revolutions. The revolution counter outputs a signal which sets the arming latch when the proper revolutions have been counted. The arming latch output goes HI to remove the reset command of the impact latch, thereby enabling the impact detector logic.

In the Super Quick mode, the selector switch is open which causes a HI input to the SQ/Delay latch at fuze power up. The SQ/Delay latch is in the reset mode, so its output is L0 which forces the U31.4 gate to a HI state. The HI output of U31.4 inputs to U31.2, so U31.2 will produce a L0 fire signal when its other input (from the impact latch) goes HI.

Fuze impact causes the impact sensor to output a positive pulse which drives the inverter L0 setting the impact latch. Both inputs to the U31.2 fire gate are HI,

# IMPACT SUPER QUICK/AUTO DELAY CIRCUIT

FIGURE 7-1



so it outputs a L0 signal which functions the fire circuit to detonate the projectile. These events describe how the impact circuit operates in the Super Quick mode.

In the Auto Delay mode, the selector switch sets the SQ/Delay latch at power up by providing low input. The latch is set at power up so loss of the selector switch at impact will have no effect on the fuze operation. The SQ/Delay latch outputs a HI signal so the U31.4 gate will enable the U31.2 fire gate as soon as the U31.3 delay gate goes L0. The impact circuit will envelope detect the pulse modulated signal generated by the impact sensor with the resistor and capacitor. When impact is detected, the impact latch is set causing one input to the U31.2 fire gate to be HI. However, the fire gate will not produce the low signal needed to function the fire circuit until the output from U31.4 goes HI. The U31.4 gate will not go HI until the output of the delay gate (U31.3) goes L0, so fuze detonation in the delay mode will occur only when the output of the delay gate goes L0.

Before impact, the output of the impact latch is L0 so the capacitor is initially uncharged and both inputs to the delay gate are L0 yielding a HI output. When impact is first detected, the output of U31.3 goes L0, setting the impact latch which charges the capacitor through the diode. The impact signal temporarily goes to zero causing the inverter to go HI, so the diode turns off and the capacitor begins to discharge through the resistor. The capacitor will not discharge because the time to discharge the capacitor is longer than the time for another impact pulse, so the output of the delay gate remains HI. The projectile continues to penetrate the targets causing additional impact sensor outputs where each impact sensor output drives the inverter L0 and recharges the



capacitor. The impact sensor will keep outputting a pulse train which continually recharges the capacitor until a target void is encountered or the projectile is stopped.

The target void or stoppage of projectile penetration causes the impact sensor to stop outputting a signal. This causes the inverter to remain HI so the diode is permanently turned off and the capacitor begins to discharge. The impact circuit produces a function delay while the capacitor discharges and the delay for the circuit presented is 0.43 mseconds. The capacitor discharges to a state where both inputs to the delay gate are HI, so the delay gate goes LO causing projectile detonation. This description explains how the impact circuit will detect a void and detonate the projectile after a fixed delay.

#### 8. Low Voltage Detector

The Low Voltage Detector (LVD) system was incorporated in the JAN fuze to realize a cleanup or backup function. This system is necessary because a fuze which misses the target and encounters soft impact will generate a signal to the impact sensor which can be insufficient for fuze detonation, so the fuze will wait for the expected valid impact signal. In the waiting mode, the fuze circuit is powered by a supply capacitor which was initially charged at setback by the environmental power supply. The supply capacitor discharges as it powers the fuze circuit and eventually will cause dudding by reaching a level which is insufficient to operate the fuze circuit. The LVD circuit prevents this type of dudding by monitoring the supply capacitor and causing fuze detonation or cleanup before the supply capacitor discharges to an insufficient level. The LVD circuit

also performs a backup function by initiating fuzes which impact a valid target, but remain undetonated due to impact sensor failure.

We selected the LVD concept for the cleanup/backup feature over a timer concept due to proven performance, accurate voltage level detection, low power needs, and simple construction of the LVD system. The alternate method to realize a cleanup/backup feature involves a timer concept. An accurate active timer can be constructed by using a crystal oscillator to drive a digital counter. The counter outputs correspond to time-outs and are monitored to cause fuze detonation at the preselected time. The disadvantage of this concept is that it requires relatively large current to operate the oscillator and the many necessary components increase system cost and volume.

A passive RC timer can primarily be constructed with a resistor, capacitor, zener diode, and comparator. The timing capacitor is charged from the fuze supply and is compared to the zener voltage reference. The time for the capacitor to charge up to the reference voltage is controlled by component values and corresponds to the desired cleanup time. This concept is disadvantageous due to the current need to bias the zener diode and the relative system inefficiency. The zener diode bias current depletes the supply capacitor and the timing capacitor charges up which further depletes the supply capacitor, leaving less supply capacitor charge to operate the fuze circuit. An alternate LVD concept was selected since it requires little bias current, contains few parts, and is currently used on various mine programs such as RAAM (Remote Artillery Antiarmor Mine).

The JAN LVD circuit is similar to the RAAM circuit and is constructed with three resistors and one transistor. The transistor is a N-Channel Enhancement Mode

MOSFET and will turn off when the gate source voltage is less than the device specified threshold. The fuze logic will reliably operate in the 3-18V range so the desired LVD switching level to ensure fuze cleanup prior to unreliable circuit operation is approximately 3.5V. The gate source switching threshold is typically in a range of 1-3 volts so a resistor divider is needed to apply a percentage of the supply voltage to the transistor gate. Resistors R1 and R2 comprise the LVD resistor divider and resistor R3 is added as a current limiter to prevent the transistor from quickly depleting the supply capacitor.

Honeywell developed the JAN LVD circuit and tested it with 3N170 and 3N171 N-Channel Enhancement Mode MOSFETS. (The 3N170 MOSFET has a switching threshold specification of 1.0-2.0 volts and the 3N171 MOSFET has a switching threshold specification of 1.5-3.0 volts.) In a functional fuze, the LVD circuit is connected to a firing element which dumps a charged capacitor into a stabber detonator which initiates the M55 detonator. We initially tested a transistor as the firing element but observed gradual turn on so a SCR was substituted. For laboratory testing, we used a 100K resistor to bleed a 500 uF charged capacitor to simulate JAN fuze capacitor discharge and a LED to indicate a low voltage detect. The circuit tested in Figure 8-1 contains a switch which was opened at  $T = 0$  to simulate the start of the 500 uF capacitor discharge and we monitored the capacitor voltage and SCR anode with an oscilloscope to document performance.

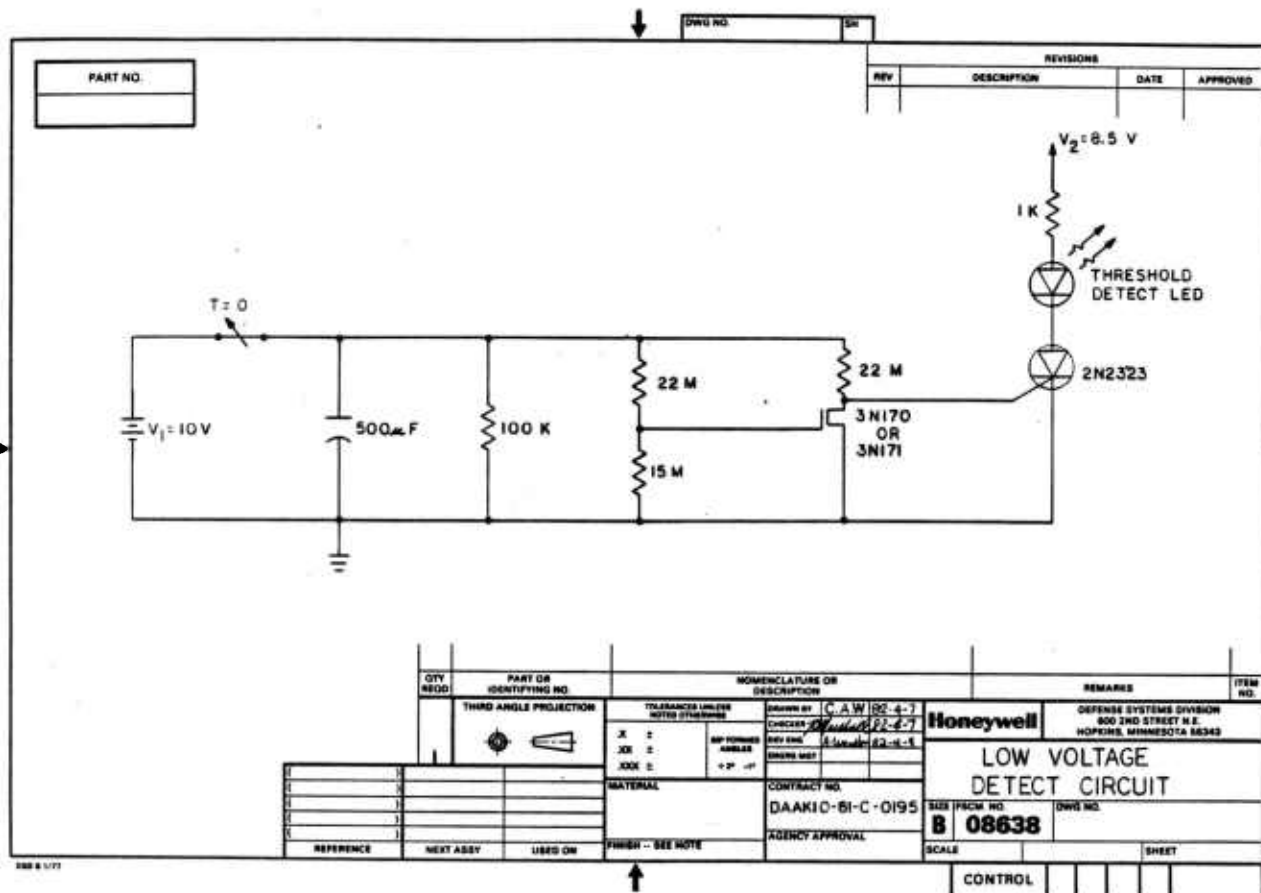
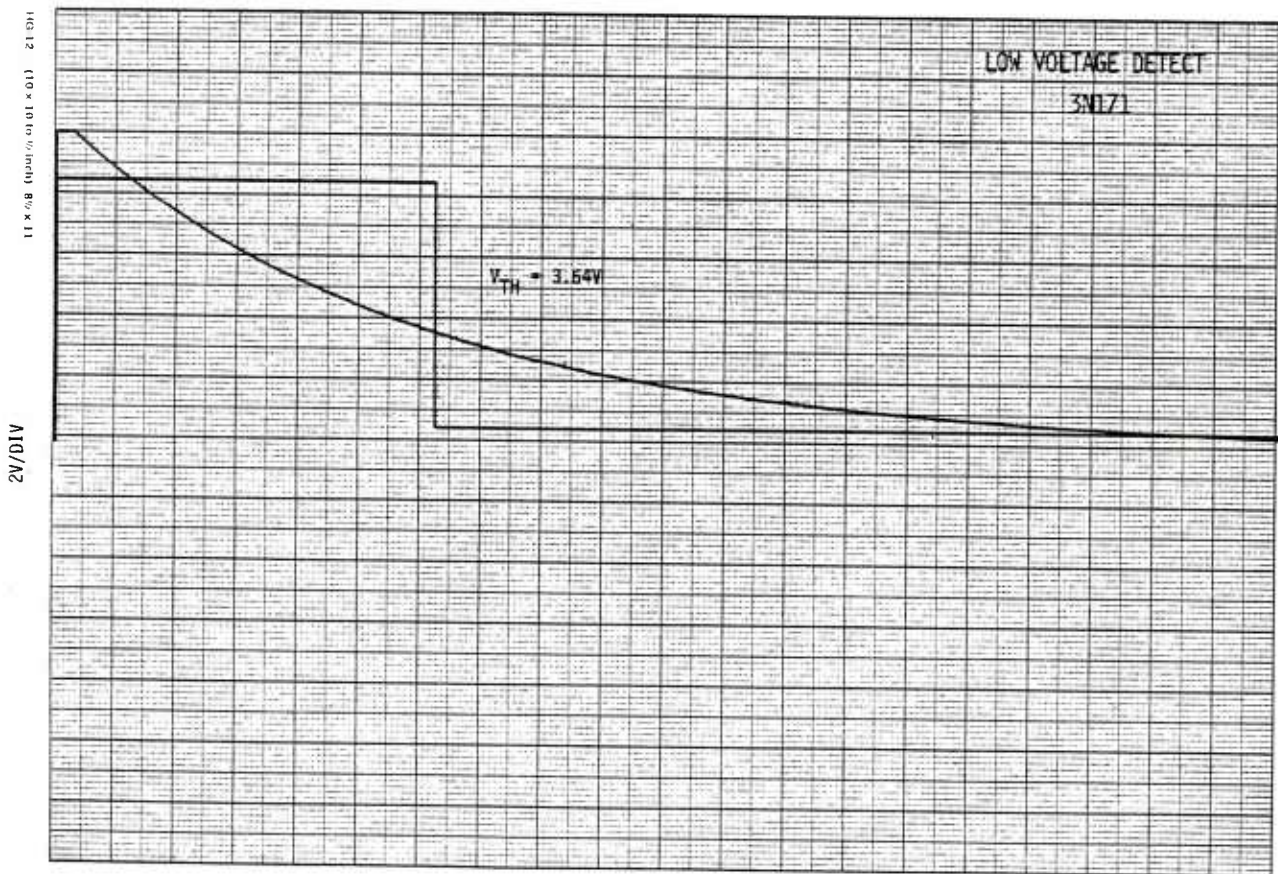
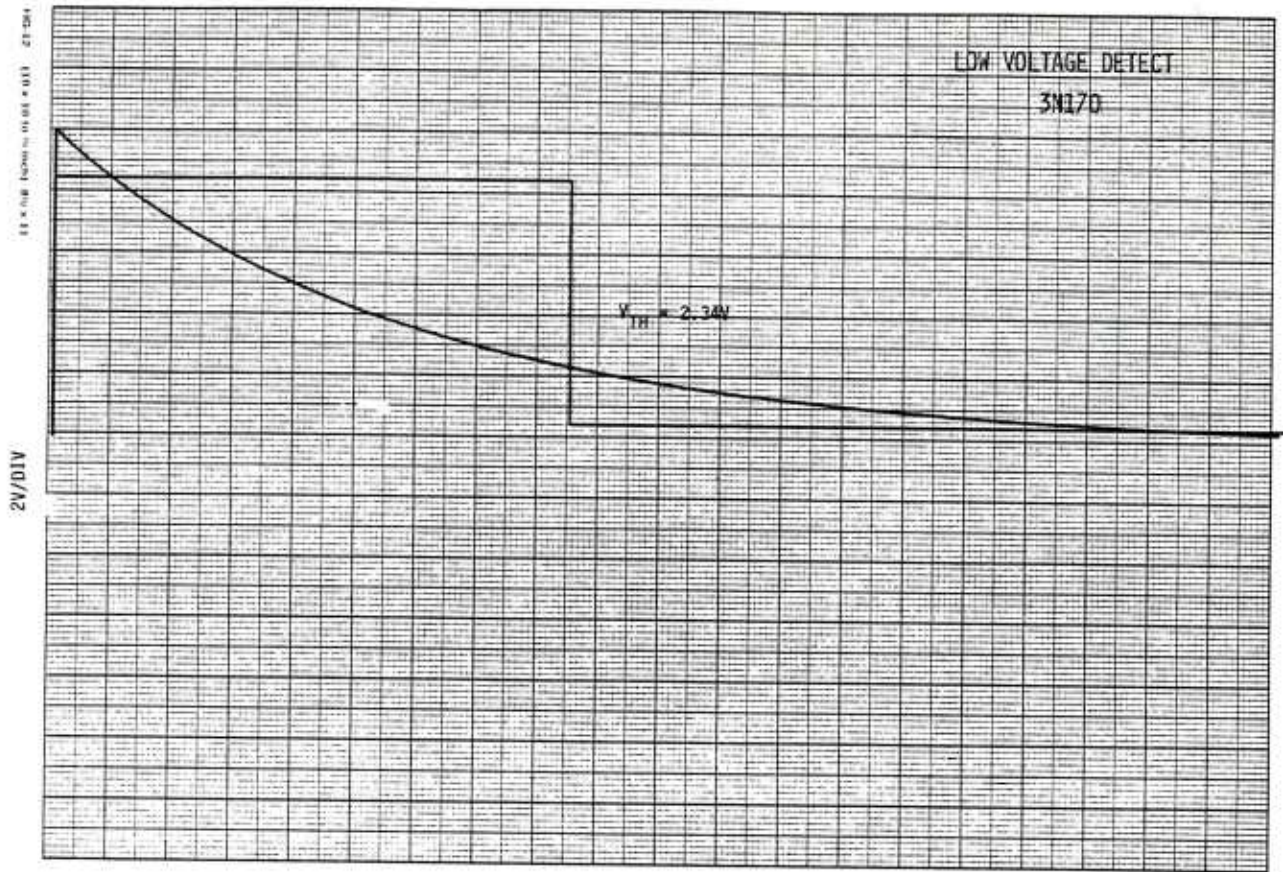


FIGURE 8-1. LOW VOLTAGE DETECTOR TEST CIRCUIT

The trace in Figure 8-2 shows the 500 uF capacitor discharged to 2.34 volts before the 3N170 turned off which caused the SCR to turn on and indicate a low voltage detect. (The exponential curve is the capacitor discharging and the second trace shows the SCR anode at  $V_2$  potential until the SCR turns on.) The trace in Figure 8-3 shows the 3N171 circuit detected a low voltage at 3.64V which is very close to the desired 3.5 threshold. The data shows it is possible to accurately detect a voltage threshold and the threshold can be adjusted by component selection. We measured the current required to operate the LVD circuit at 0.66 uA and could further reduce it by increasing the resistor values. This data demonstrates that it is possible to construct an accurate low power low voltage detector.





10 SEC/DIV  
Figure 8-3 3N170 LVD DATA

## 9. Demonstrator

Honeywell constructed a model to demonstrate the JAN fuze electronic environmental sensors. The demonstrator is a battery-powered unit which contains a setback sensor, revolution sensor, impact sensor, and control box with a display panel. The demonstrator, Figure 9-1, is used to independently demonstrate the environments which are electronically evaluated by the Electronic JAN PD/D fuze.

The model can be used to demonstrate the setback sensor concept by dropping the setback weight on the sensor and watching the setback indicator LED. The setback weight is a metal rod which has a rubber foot and grommet attached to one end. The metal end produces a short pulse typical of accidental forty-foot drops and the rubber end produces a long pulse typical of actual setback acceleration. The setback tube has an all arm line which corresponds to the all arm Army requirement of 600 g's and a no arm line which corresponds to the no arm 400 g requirement.

The setback sensor concept is demonstrated by dropping the weight on the sensor at various heights to simulate various setback accelerations. When the user drops the rubber end setback weight from a height above the all arm line, the indicator LED will light to indicate an accepted pulse. Dropping the rubber end setback weight below the no arm line causes the indicator LED not to light which demonstrates pulse rejection. The user can drop the metal end setback sensor from any height, but the circuit will reject this pulse as evident by the LED staying off. (The circuit, Figure 9-2, is similar to the one used in shock tower testing.) The model demonstrates that the setback sensor will reject forty-foot drops and only accept drops with the required amplitude and pulse duration.

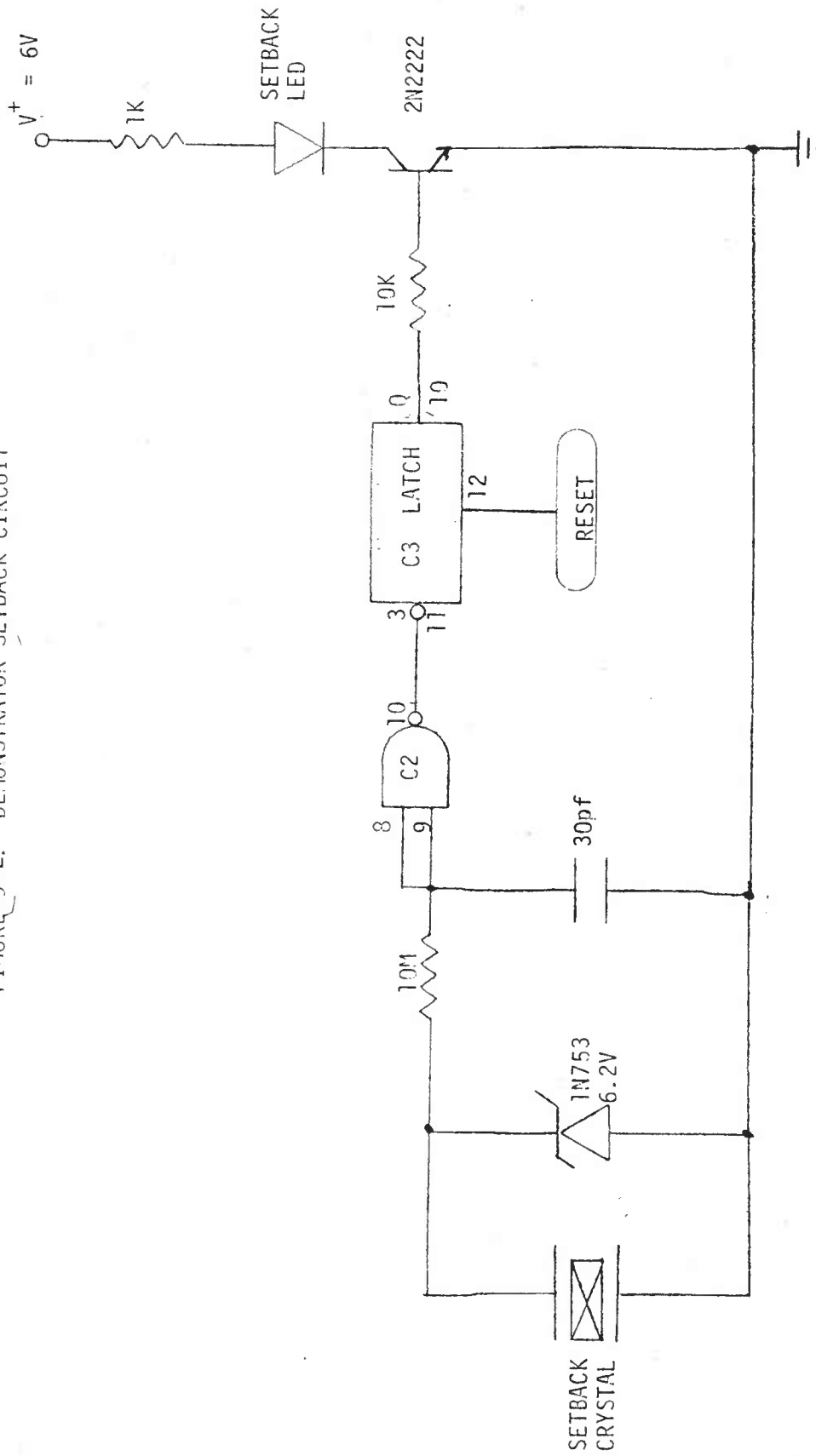


FIGURE 9-1 DEMONSTRATOR





FIGURE 9-2. DEMONSTRATOR SETBACK CIRCUIT



The second environment our model demonstrates is revolution sensing. We constructed a hand-held unit by mounting a pole piece sensor and amplifier to a motor driven shaft. A 6000 turn #44 wire pole piece sensor was connected to the amplifier used in revolution testing and mounted on an aluminum shaft inside a plexiglass ogive. A variable speed motor spins the shaft to simulate the revolving of a projectile.

The hand-held unit is connected to the control box which contains the motor speed control circuit, spin rate detector, revolution counter, and display LED's. The spin rate LED will blink as a function of revolutions if the spin rate is above a 400 rpm threshold. Any revolutions above the threshold are counted and the 32 count LED will turn on when 32 revolutions have been counted. The revolution sensor circuit, Figure 9-3, can determine proper spin rate and count a fixed number of revolutions. The model is therefore used to demonstrate how the JAN fuze determines spin rate to function EBM bolt 2 and counts revolutions which corresponds to fixed safe separation distance to fire EBM bolt 3.

The final environment the JAN fuze model demonstrates is impact. Once the JAN fuze has detected proper setback, revolution spin rate and number of revolutions, it has functioned EBM bolts 1, 2, and 3 respectively. The fuze is now armed and will function in the Super Quick or Auto Delay mode at impact.

The user selects the demonstrator Super Quick or Auto Delay option with the selector switch and simulates impact by tapping the impact sensor with the hammer. In the Super Quick mode, the impact circuit, Figure 9-4, will accept the first impact pulse and immediately turn the impact LED on to demonstrate Super Quick detonation. In the Auto Delay mode, the circuit will wait until

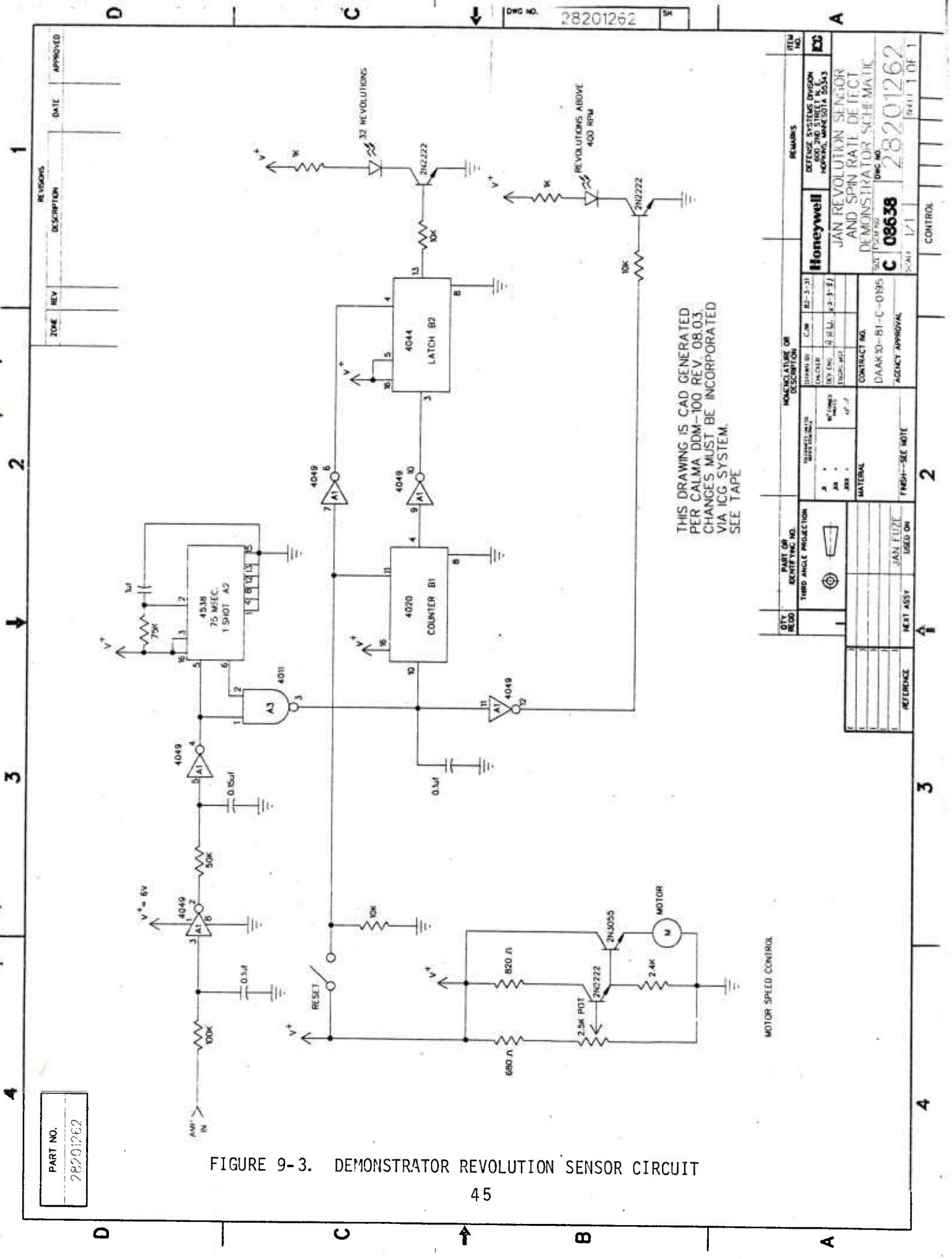


FIGURE 9-3. DEMONSTRATOR REVOLUTION SENSOR CIRCUIT

PART NO.  
28201262

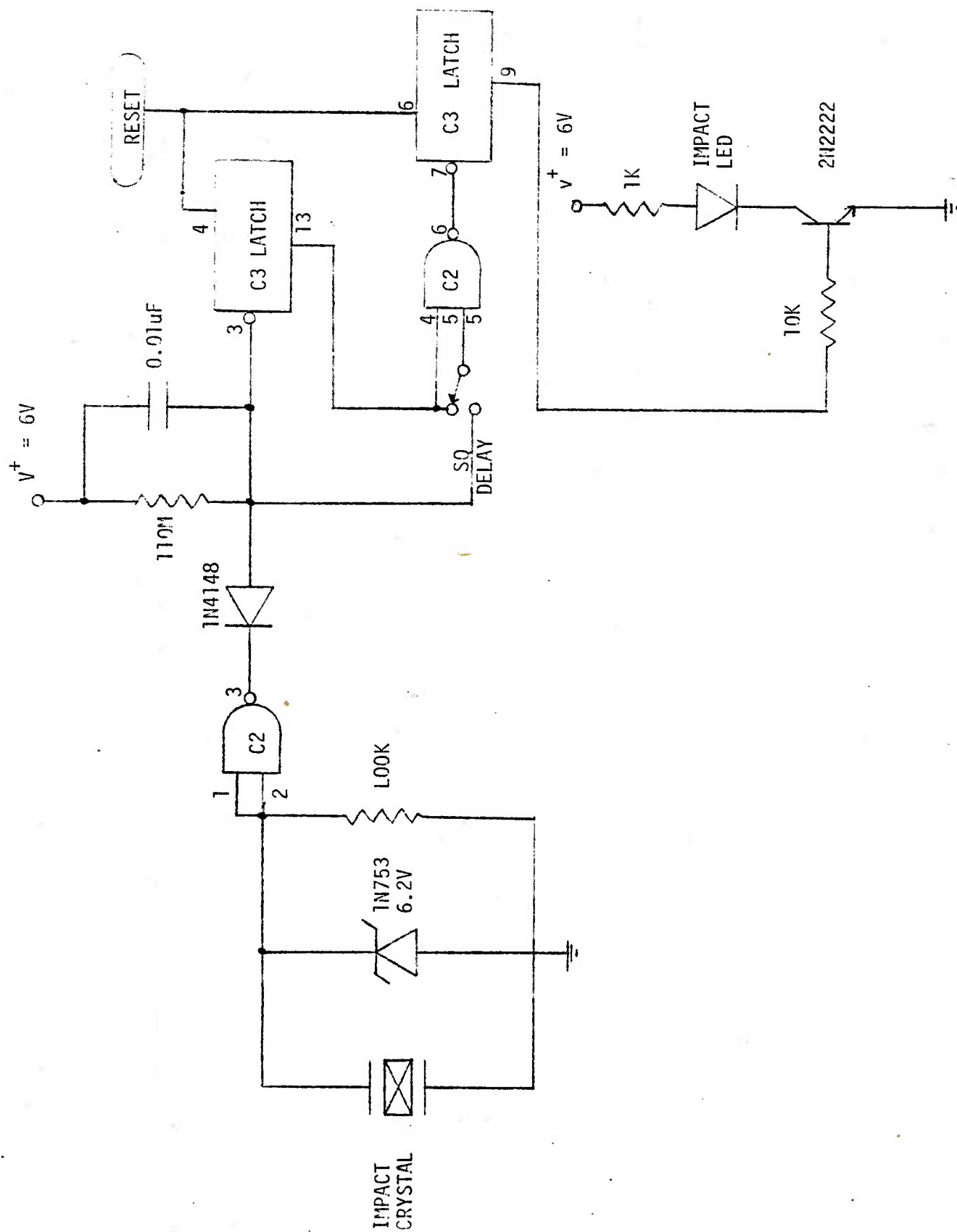
ZONE	REV	DESCRIPTION	DATE	APPROVED

QTY REQD		PART OR IDENTIFYING NO.		NOMENCLATURE OR DESCRIPTION		REMARKS	
THIRD ANGLE PROJECTION		THIRD ANGLE PROJECTION		THIRD ANGLE PROJECTION		THIRD ANGLE PROJECTION	
MATERIAL		MATERIAL		MATERIAL		MATERIAL	
FINISH-SEE NOTE		FINISH-SEE NOTE		FINISH-SEE NOTE		FINISH-SEE NOTE	
REFERENCE		REFERENCE		REFERENCE		REFERENCE	
NEXT ASSY		NEXT ASSY		NEXT ASSY		NEXT ASSY	
USED ON		USED ON		USED ON		USED ON	
JAN FLUZE		JAN FLUZE		JAN FLUZE		JAN FLUZE	
CONTROL		CONTROL		CONTROL		CONTROL	
PAGE 1 OF 1		PAGE 1 OF 1		PAGE 1 OF 1		PAGE 1 OF 1	

Honeywell  
 JAN REVOLUTION SENSOR  
 AND SPIN RATE DE FEET  
 DEMONSTRATOR SCHEMATIC  
 C 08638  
 28201262  
 1/1

MOTOR SPEED CONTROL

FIGURE 9-4. DEMONSTRATOR IMPACT CIRCUIT



penetration, simulated by quick repetitive tapping, has stopped and then add a short delay before impact LED turn on. This feature demonstrates the void sensing with delay concept previously discussed in the impact sensor section.

The JAN fuze model will individually demonstrate all the environmental sensing concepts. The complete JAN fuze electronics would be constructed by adding power supply and fire circuits to sensor electronics similar to those used in the JAN fuze demonstrator model.

#### 10. Power Supply Task

The two part power supply task was the only program objective we did not complete. A simulated power supply test was to be conducted where a breadboard fuze would be powered from a capacitor and function microdetonators to simulate the Electro Explosive Devices contained in the Explosive Barrier Module (EBM) S&A. This test would indicate the JAN fuze electronic circuit could operate from the environmental power supply and properly function the S&A. Positive simulated power supply performance was to result in conducting of the actual power supply tests. The actual power supply tests would be conducted by using a setback generator power supply to operate the breadboard fuze electronics which would function an EBM. Positive results from this test would demonstrate the feasibility of the Electronic JAN PD/D fuze concept from a power supply standpoint.

The power supply tests were not conducted due to EBM program uncertainty and lack of hardware. We were concurrently funded to develop the EBM concept when this Electronic JAN PD/D fuze program began, but the EBM program was completed and a



follow-up program was not scheduled for us. The EBM program concluded at a state where the hardware would not reliably operate as designed, so the use of an Explosive Barrier Module for the JAN fuze S&A is uncertain (HDL is conducting a follow-on program, but program status is currently unknown by Honeywell). Program engineers did not conduct the power supply tests due to the lack of EBM hardware and uncertainty of the EBM concept. We applied the funds allocated for power supply testing to additional subsystem development which resulted in optimum use of all program funding.

#### 11. Electronic S&A

Honeywell proposed that the Explosive Barrier Module be used in the Electronic JAN PD/D fuze as the Safing and Arming device. The Explosive Barrier Module was designed to enable fuze arming once three independent environments were acceptably detected. We planned to operate the Explosive Barrier Module from the setback, revolution spin rate, and number of revolution environments previously discussed.

The Explosive Barrier Module program concluded with uncertain results so an alternate Safing and Arming concept may be needed for the Electronic JAN fuze. This section contains a discussion of the Explosive Barrier Module program and a Honeywell Internal Development Electronic Safing and Arming program. We did not expend any effort on the JAN fuze S&A under this contract and are including this Electronic S&A discussion only to present a more complete understanding of the total Electronic JAN PD/D fuze concept.

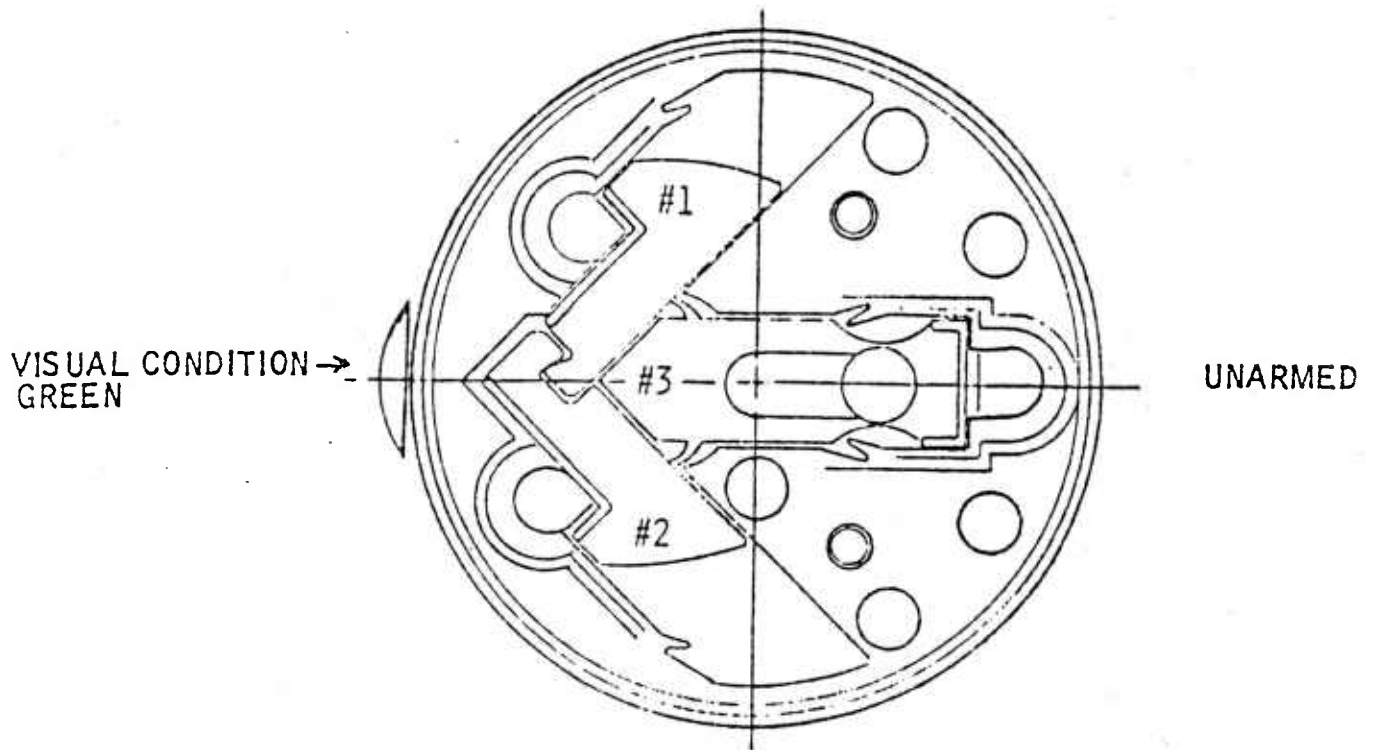
### 11.1 Explosive Barrier Module

The Explosive Barrier Module (EBM) is the element of the JAN fuze Safing and Arming (S&A) device which provides out-of-line explosive train interruption. The EBM incorporates three movable members (bolts), mechanically interlocked so that they can move in only one predetermined sequence, with movement of the third member arming the device, see Figure 11-1. Propellant charges are electrically initiated by the fuze electronics to provide the force to move the bolts into the armed positions.

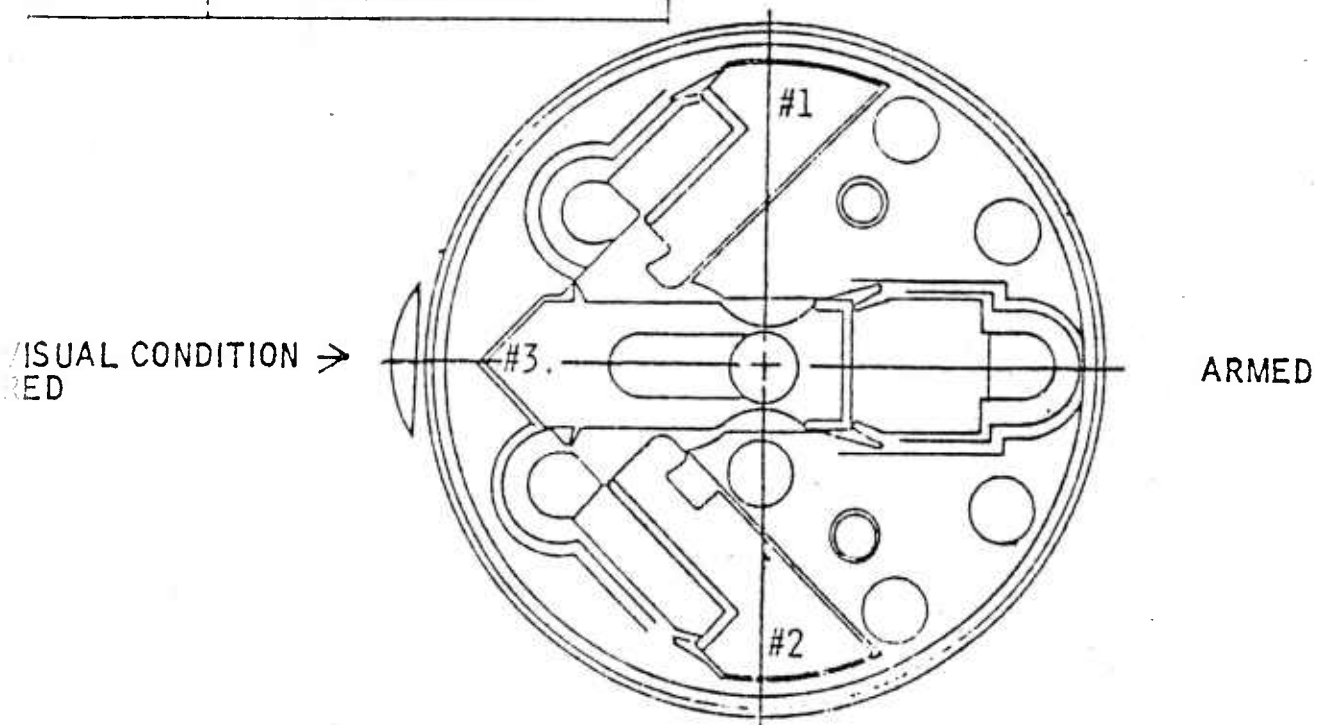
The EBM achieves safety during prelaunch by using a mechanical interlock to lock each movable bolt to the others and to the EBM housing. The housing interlock consists of a shear pin on each bolt which must be sheared to move the bolt from the safe position. The shear pin is designed to maintain the bolt in the safe position under a side load of up to 20,000 G's.

The arming cycle is accomplished by reaction to three sequential electric signals received from the JAN fuze electronics. Each electric signal will initiate a propellant charge which provides the force to shear the pin and move the respective bolt. Movement of the third bolt will arm the device by positioning an M55 stab detonator between a fourth propellant charge and a lead charge. The third bolt positively locks in the EBM in the armed position. A firing pin rides with the third bolt and is positioned on the sensitive end of the M55 stab detonator. The firing pin is driven by the fourth pyrotechnical propellant charge to reliably initiate the stab detonator.

FIGURE 11-1  
EXPLOSIVE BARRIER MODULE (EBM)



EBM FUNCTION	ENVIRONMENT
BOLT #1	SETBACK
BOLT #2	RATE OF SPIN
BOLT #3	SAFE SEPARATION
DET	IMPACT/AUTO DELAY



## 11.2 Internal Development Program

Honeywell has been developing the technologies required for an all electronic artillery fuze through Internal Development and DOD funded programs. We have been pursuing the electronic fuze for over two decades and our effort has involved fuze concept definition and field testing of electronic environmental sensors. The major obstacle of the electronic fuze has been the development of a solid state or electrically functioned S&A which can meet the strict safety requirements the Department of Defense and Honeywell are committed to. However, we believe the technology exists today to develop a state-of-the-art electronic S&A for use in all electronic JAN fuze.

The Explosive Barrier Module was one concept we investigated and additional development may result in a device suitable for the Electronic JAN fuze. Honeywell has defined other solid state S&A concepts which include electrical, explosive summing, shock aiding, and shock inhibiting S&A approaches. Alternate concepts which may be suitable for the Electronic JAN fuze include a laser initiated explosive train, exploding bridge wire, and slapper detonator S&A approaches.

The acceptance of electronic systems in today's weapons is growing as evident by the electronic-mechanical S&A systems used in various systems such as Copperhead, FAE-II, SLUFAE, and the Advanced Lightweight Torpedo. The realization of an electronic S&A is within today's technology domain and we are committed to working towards this goal. Additional support and development of the electronic S&A concepts is needed so the realization of the Electronic JAN PD/D fuze can occur.

## 12. Fuze Packaging

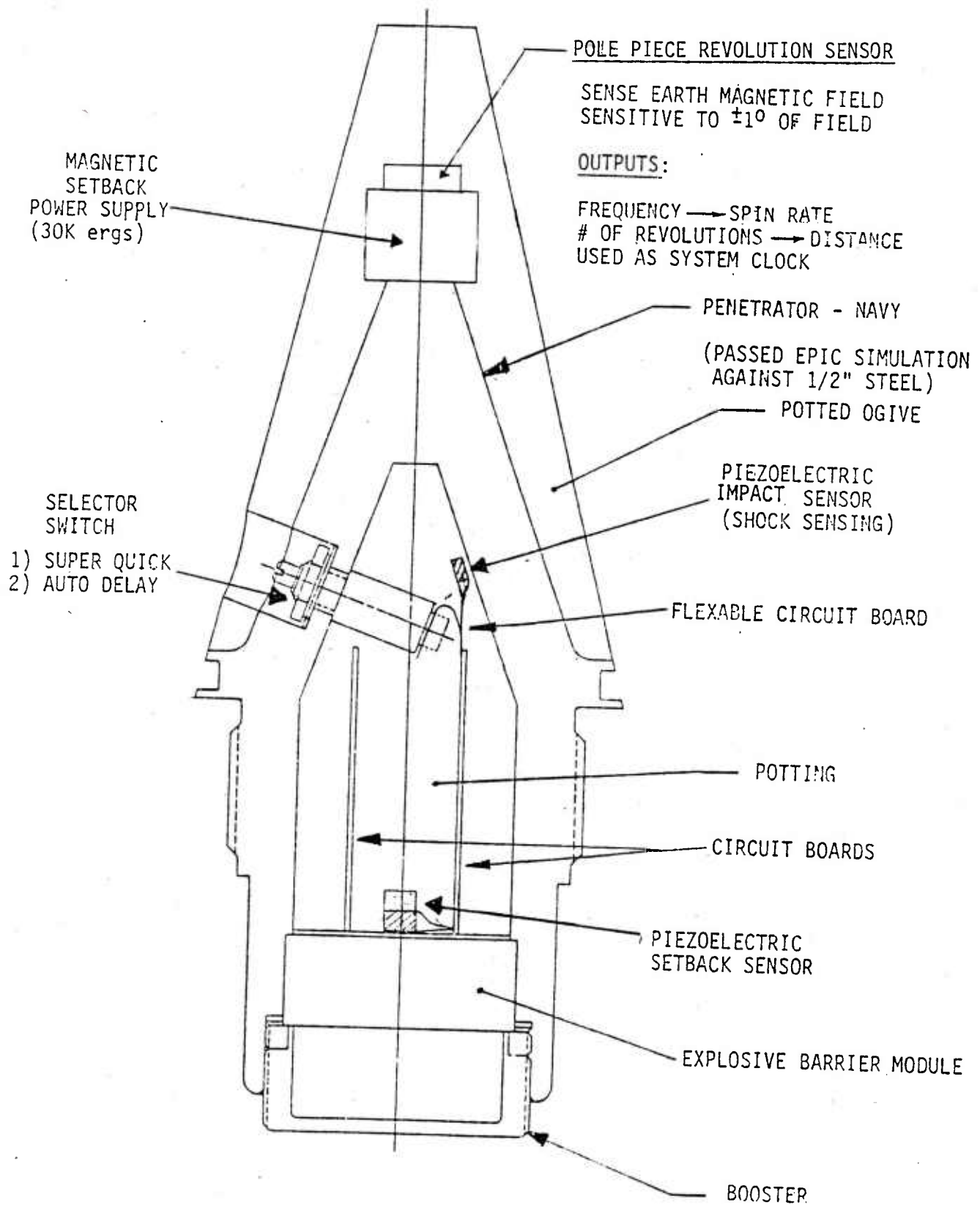
Mechanical engineers developed individual Army and Navy penetrator designs in the 1980 program. We designed both fuzes with identical penetrator cavities for maximum fuze commonality. We presented a drawing for the JAN fuze which detailed where the electronic circuit board, magnetic power supply, revolution sensor coils, selector switch, and EBM would be mounted. Honeywell has prepared Figure 12-1, which is similar to the previous drawing, with the exception of the pole piece. We substituted the pole piece for the magnetic sense coils because this device was selected for the JAN revolution sensor. The pole piece is mounted directly above the environmental power supply and is secured by the potting compound.

## 13. Conclusion

Honeywell has made good progress on this continued exploratory development program. We completed shock tower testing which demonstrated that our setback sensor does conform to the Army all arm and no arm setback requirements. We conducted extensive revolution sensor testing which resulted in the selection of a small, sensitive, low cost pole piece revolution sensor for the JAN PD/D fuze. We also performed testing to demonstrate how a low voltage detector circuit can sense a low voltage level and output a detonate signal to realize a projectile cleanup feature. We jointly conducted a programmable feasibility task with the Naval Surface Weapons Center and concluded that additional development is needed to yield a device which can double as a revolution sensor and magnetic receiver link for use on a Multi-Option Fuze. We fabricated a JAN PD/D fuze demonstrator model to demonstrate the setback, revolution spin rate detector, revolution



FIGURE 12-1  
JAN ELECTRONIC PD/D FUZE



counter, and impact features of the fuze. The model will be used to independently demonstrate the environmental sensing techniques of the JAN PD/D fuze.

Program engineers completed all the program objectives except the power supply tests. The power supply tests were included as a program objective to demonstrate the feasibility of using the environmental power supply to function the JAN fuze system, but we did not conduct these tests because of marginal Explosive Barrier Module program results. The marginal EBM program results indicated that the selection of the EBM for the JAN fuze S&A must be reviewed, so we tested those concepts which are definitely part of the Electronic JAN PD/D fuze.

We have demonstrated feasibility of most electronic subsystems of the JAN PD/D fuze. We have not encountered any unsolvable problems, so the Electronic JAN PD/D fuze concept is ready for further development.

#### 14. Recommendations

The Electronic JAN Point Detonating/Delay fuze environmental sensors have been developed to a state where they are ready for field testing. Honeywell recommends that fuzes be gun fired to confirm the feasibility of measuring safe separation distance by counting projectile revolutions. We suggest several fuzes be constructed with a pole piece revolution sensor, revolution spin rate detector, revolution counter, and flash charge. The fuzes will be battery powered and will use an existing S&A, such as an M739. We recommended that the fuzes be fired at various zones and high-speed cameras be used to collect data to verify theoretical versus actual performance.

The second level of field tests would involve the setback sensor. The setback sensor would be added to the safe separation fuze if the safe separation test data is acceptable. The setback pulse would electrically arm the projectile and the flash charge would be initiated at the proper safe separation distance. This test would demonstrate the setback and safe separation concepts.

We recommend a final level of field tests to demonstrate the impact sensor capability of the JAN fuze. A flash charge would be initiated upon impact in the super quick mode to demonstrate this feature. To demonstrate the Auto Delay mode, the fuze would penetrate several plywood targets and initiate a flash charge after a short delay. This test would demonstrate how the impact circuit can operate as a void sensor with short delay. High-speed photography would be used to document fuze performance.

We have also identified other areas for additional work. The Army penetrator needs additional development before it will pass the EPIC computer simulation, but the Navy penetrator passed when tested in the previous JAN fuze program. Several Navy penetrators could be constructed and shot at targets to determine penetration performance. A similar test could be conducted with a redesigned Army penetrator and acceptable results in this area would lead to accepted penetrator designs for the JAN fuze.

The final area we recommend for future work is the Electronic S&A. An acceptable S&A is a necessity for the JAN fuze and effort in this area is paramount for realization of the total fuze concept. Progress from the development currently being conducted on the Explosive Barrier Module by HDL should be monitored and power supply tests should be conducted when the EBM feasibility is demonstrated.

These tests would show electrical power supply feasibility for an acceptable JAN fuze system which uses the EBM as the system S&A.

Honeywell has identified many areas for future JAN fuze program effort. At a minimum, we recommend that the gun firing tests be conducted to demonstrate feasibility of counting fuze revolutions to discern safe separation distance. We have presented several other areas which can be independently developed. Effort in all areas will be required before the total Electronic JAN PD/D fuze concept can be established.

## APPENDIX A

### PIEZOELECTRIC SETBACK SENSOR PROGRAM FOR A HP-41C



## Piezoelectric Setback Sensor Program for a HP-41C

by Alan Wendler

Aug. 20, 1981

### Abstract

A setback sensor can be constructed using a cylindrical piezoelectric (pz) crystal with an equal diameter weight placed above it. Electrical contact is made to both sides of the pz crystal and upon setback, the weight will mechanically stress the pz crystal which produces a voltage proportional to the amount of setback. This report describes a HP-41C calculator program which will calculate the output voltage for a particular set of conditions.

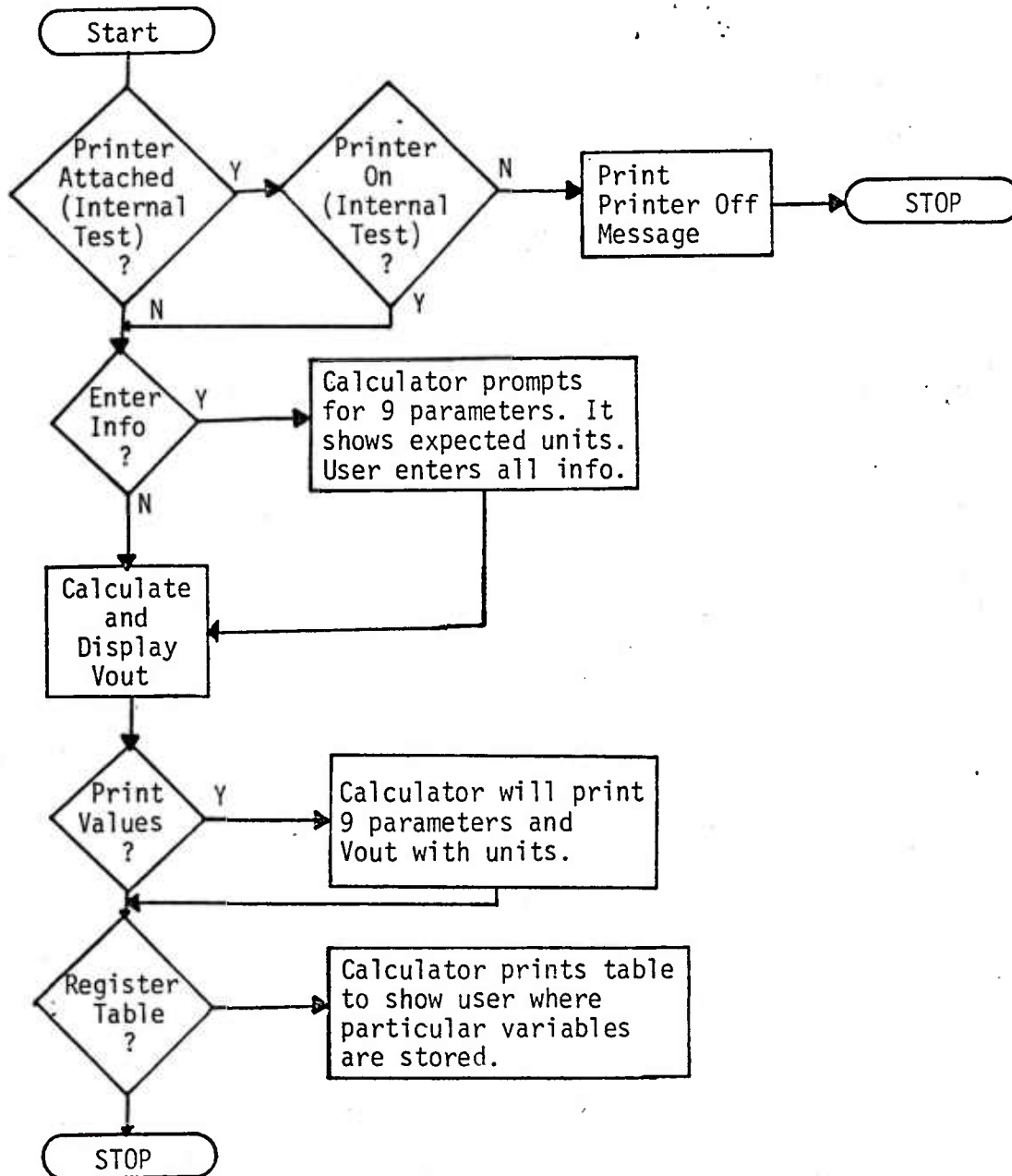
### Introduction

When designing a piezoelectric setback sensor, output voltages are calculated for various parameters and it is necessary to have a program that can calculate  $V_{out}$  for one set of parameters, easily accommodate a change in any particular parameter, then recalculate  $V_{out}$  so the user can determine what effect specific parameter changes have on  $V_{out}$ .

This program gives the user the option of initializing all information, printing all values and printing the register table. The program can be used with printer so parameters and results are easily documented, but a printer is not required.

Once the calculator outputs  $V_{out}$ , the user may stop execution, change a value, and start the program over. This enables the user to quickly determine  $V_{out}$  with minimal button pushing, but all options are available if the user wants them.

# Piezoelectric Setback Sensor Program Flowchart



### Calculator Program

The calculator determines  $V_{out}$  from the equation derived on page 63 and A program listing is given on page 65. - The program determines if a printer is connected and turned on. If an attached printer is off, a "printer off" message is output.

The program first prompts the user with "Enter Info (Y/N)?" If the user simply wants to calculate  $V_{out}$  for the parameters stored in registers R1-R9, then inputting a "N" will cause the  $V_{out}$  to be calculated and displayed. If the user wants to input all info, then typing a "Y" will cause nine prompts to appear. The program asks for setback level (G's), the external load capacitance (farads), the pz crystal diameter (inches), the pz crystal length (inches), the pz  $e_o$  constant (coulomb/cm volt), pz D33 constant (coulomb/newton), the length of the weight (inches), the density of the weight (lb/cubic inch), and the weight type. The weight type is the name of the metal, such as steel. The program then computes and outputs  $V_{out}$ .

At this time, the program will pause and the user may stop the program, change a parameter, and recalculate  $V_{out}$ . If the user does not stop execution, the program will prompt with "PR values (Y/N)?". If the user wants all parameters or values printed, entering a "Y" will cause the program to print all values with their units. This feature is useful with a printer to document the result that particular parameters give.

The program will then prompt with "REG TABLE?" entering a "Y" will cause the register table to be printed.

### Register Table

R1 = setback

R2 = ext cap

R3 = PZ diameter

R4 = PZ length

R5 = PZ  $\epsilon_0$

R6 = PZ D33

R7 = wt length

R8 = wt density

R9 = wt type

R10 = Vout

This is a reference for the user so he knows where the particular parameters are stored. This is helpful when the user varies a particular parameter and runs the program to find Vout. The first time the program is used, all information will be entered and Vout will be output. The user may stop execution, change R1 from 550 G's to 3000 G's, and rerun the program. Vout is now calculated using 3000 G's.

Sample Run

Determine the voltage generated when a setback sensor, comprised of a 0.2" diameter x .132" long crystal and same size steel weight, experience 550 g's of setback acceleration.

$$d_{33} = 350 \times 10^{-12} \text{ C/N}$$

$$e_0 = 142 \text{ pcoul/cm volt}$$

$$P_{\text{steel}} = 0.28 \text{ lb/cu in}$$

Assume no external capacitance

Answer:  $V_{\text{out}} = 11.57 \text{ volts}$

```

ENTER INFO<Y/N>?
Y                                RUN
SETBACK<G>?
550                             RUN
EXT CAP<F>?
0                               RUN
PZ DIAMETER<IN>?
.2                              RUN
PZ LENGTH<IN>?
.132                           RUN
PZ e.<COUL/CM VOLT>?
142-12                         RUN
PZ D33<COUL/N>?
350-12                         RUN
WT. LENGTH<IN>?
.132                           RUN
WT. DENSITY<LB/CU IN>?
.28                            RUN
WT. TYPE?
STEEL                           RUN
V OUT=11.57E0 VOLTS
PR VALUES<Y/N>?
Y                                RUN

```

```

SETBACK=550.0E0 G
EXT CAP=0.000E0 F

```

```

CRYSTAL INFO
DIAMETER=200.0E-3 IN
LENGTH=132.0E-3 IN
e.=142.0E-12COUL/CM V
D33=350.0E-12 COUL/N

```

```

STEEL WEIGHT
LENGTH=132.0E-3 IN
DENSITY=280.0E-3LB/CU IN

```

```

V OUT=11.57E0 VOLTS
REG TABLE?
Y                                RUN

```

```

REGISTER TABLE
R1=SETBACK
R2=EXT CAP
R3=PZ DIAMETER
R4=PZ LENGTH
R5=PZ e.
R6=PZ D33
R7=WT LENGTH
R8=WT DENSITY
R9=WT TYPE
R10=V OUT

```

```

3000 STO 01
XEQ "SETBACK"

```

Determine  $V_{\text{out}}$  if we have 3000 g's of setback

Answer:  $V_{\text{out}} = 63.14 \text{ volts}$

```

ENTER INFO<Y/N>?
N                                RUN
V OUT=63.14E0 VOLTS
PR VALUES<Y/N>?
N                                RUN
REG TABLE?
N                                RUN

```

## EQUATION DERIVATION

For a Piezoelectric Crystal:

Charge = Total Capacitance x Voltage

$$Q = C_T V \quad (1)$$

Total Capacitance = Capacitance of pz. crystal + external load capacitance

$$C_T = \frac{\epsilon_0 A}{L_{pz}} + C_{ext}$$

$$C_T = \frac{\epsilon_0 \pi (d_{pz})^2}{4 L_{pz}} + C_{ext} \quad (2)$$

Also

Charge = Force on Crystal x Crystal Sensitivity

$$Q = F d_{33} \quad (3)$$

Where

Force = Mass x Acceleration

$$F = ma$$

$$= \frac{\pi d^2}{4} \times L_{wt} \times \rho_{wt} \times setback \times a \quad (4)$$

Combining 1 and 3 we get:

$$V_{out} = \frac{F d_{33}}{C_T}$$

Substituting 2 and 4 and performing a dimensional analysis, we get:

$$V_{out} = \frac{\frac{\pi (d_{pz})^2}{4} \times L_{wt} \times \rho_{wt} \times setback \times \left(\frac{9.80m}{sec^2}\right) \times \left(\frac{.4536 kg}{1b}\right) \times d_{33}}{\frac{\pi (d_{pz})^2 \times \epsilon_0 \times \left(\frac{2.54cm}{in}\right) + C_{ext}}{4 \times L_{pz}}}$$



Where:  $V_{out}$  -- output voltage (volts)

$d_{pz}$  -- diameter of pz crystal (inches)

$L_{wt}$  -- length of weight (inches)

$\rho_{wt}$  -- density of weight (lb/cubic inch)

setback -- number of g's experienced at setback

$D_{33}$  -- pz crystal sensitivity constant (coulombs/newton)

$\epsilon_0$  -- pz crystal material constant (coulombs/cm volt)

$L_{pz}$  -- length of pz crystal (inches)

$C_{ext}$  -- external parallel crystal load capacitance (farads, may equal 0)

# PROGRAM LISTING

```

01*LBL "SETBACK"
02 ENG 3
03 CLA
04 FS? 55
05 PRA
06 AON
07 "ENTER INFO<Y/N>"
08 "I?"
09 PROMPT
10 ASTO X
11 AOFF
12 "Y"
13 ASTO Y
14 X=Y?
15 XEQ 01
16 XEQ 02
17 "V OUT="
18 ARCL 10
19 "I VOLTS"
20 AVIEW
21 PSE
22 PSE
23 CLA
24 AON
25 "PR VALUES<Y/N>?"
26 PROMPT
27 ASTO X
28 AOFF
29 "Y"
30 ASTO Y
31 X=Y?
32 XEQ 03
33 CLA
34 AON
35 "REG TABLE?"
36 PROMPT
37 ASTO X
38 AOFF
39 "Y"
40 ASTO Y
41 X=Y?
42 XEQ 04
43 CLX
44 RTN
45*LBL 01
46 "SETBACK<G>?"
47 PROMPT
48 STO 01
49 "EXT CAP<F>?"
50 PROMPT
51 STO 02
52 "PZ DIAMETER"
53 "I<IN>?"
54 PROMPT
55 STO 03
56 "PZ LENGTH"
57 "I<IN>?"
58 PROMPT
59 STO 04
60 "PZ e.<COUL/CM V"
61 "I<OLT>?"
62 PROMPT
63 STO 05
64 "PZ D33<COUL/N>?"
65 PROMPT
66 STO 06
67 "WT. LENGTH<IN>?"
68 PROMPT
69 STO 07
70 "WT. DENSITY<LB/"
71 "I<CU IN>?"
72 PROMPT
73 STO 08
74 AON
75 "WT. TYPE?"
76 PROMPT
77 ASTO 09
78 AOFF
79 RTN
80*LBL 02
81 RCL 03
82 2
83 /
84 X12
85 PI
86 *
87 STO 12
88 RCL 07
89 *
90 RCL 08
91 *
92 RCL 01
93 *
94 9.88
95 *
96 .4536
97 *
98 RCL 06
99 *
100 STO 11
101 RCL 12
102 ENTER↑
103 RCL 05
104 *
105 ENTER↑
106 2.54
107 *
108 RCL 04
109 /
110 RCL 02
111 +
112 1/X
113 RCL 11
114 *
115 STO 10
116 RTN
117*LBL 03
118 CLA
119 AVIEW
120 "SETBACK="
121 ARCL 01
122 "I G"
123 XEQ 06
124 "EXT CAP="
125 ARCL 02
126 "I F"
127 XEQ 06
128 AVIEW
129 "CRYSTAL INFO"
130 XEQ 06
131 "DIAMETER="
132 ARCL 03
133 "I IN"
134 XEQ 06
135 "LENGTH="
136 ARCL 04
137 "I IN"
138 XEQ 06
139 "e.="
140 ARCL 05
141 "I<COUL/CM V"
142 XEQ 06
143 "D33="
144 ARCL 06
145 "I< COUL/N"
146 XEQ 06
147 AVIEW
148 ARCL 09
149 "I< WEIGHT"
150 XEQ 06
151 "LENGTH="
152 ARCL 07
153 "I IN"
154 XEQ 06
155 "DENSITY="
156 ARCL 08
157 "I<LB/CU IN"
158 XEQ 06
159 AVIEW
160 "V OUT="
161 ARCL 10
162 "I VOLTS"
163 AVIEW
164 PSE
165 RTN
166*LBL 04
167 CLA
168 AVIEW
169 "REGISTER TABLE"
170 XEQ 06
171 "R1=SETBACK"
172 XEQ 06
173 "R2=EXT CAP"
174 XEQ 06
175 "R3=PZ DIAMETER"
176 XEQ 06
177 "R4=PZ LENGTH"
178 XEQ 06
179 "R5=PZ e."
180 XEQ 06
181 "R6=PZ D33"
182 XEQ 06
183 "R7=WT LENGTH"
184 XEQ 06
185 "R8=WT DENSITY"
186 XEQ 06
187 "R9=WT TYPE"
188 XEQ 06
189 "R10=V OUT"
190 AVIEW
191 PSE
192 RTN
193*LBL 06
194 AVIEW
195 PSE
196 CLA
197 RTN
198 END

```

## APPENDIX B

### PZ VOLTAGE TABLE PROGRAM FOR THE HP-41C

## PZ Voltage Table Program for the HP-41C

by Alan Wendler

September 9, 1981

### Abstract

This report describes a calculator program written to supplement another calculator program, which was described in the authors August 20, 1981 report entitled "Piezoelectric Setback Sensor Program for a HP-41C". This program will generate a voltage table, where pz output voltage is printed for values of load capacitance and setback G's. This report assumes the reader is familiar with the previous report and piezoelectric setback sensors.

### Introduction

This program was written so the user could specify one to four setback levels, and a large number of load capacitor values. The program will generate a table where the output voltage is calculated as a function of particular setback and load capacitance values. The user must initially store the parameters in the calculator registers, and then execute the program to generate the table. The program uses registers 10 to 35 for a table with four load capacitor values, and one additional register beyond register 35 for every additional load capacitor value beyond four.

### User Input

The user must initialize the following registers with the following information:

R10-R18 used internally

R19 number of setback values to be used (1-4)

R20 pz diameter (inches) note: program assumes wt. diameter =  
pz. diameter

R21 pz length (inches)

R22 weight length (inches)

R23  $D_{33}$  (coul/newton)

R24  $\epsilon_0$  (coul/cm volt)

R25 weight name (Alpha date - i.e., steel)

R26 weight density (lb/cu. in.)

R27 setback value #1

R28 setback value #2

R29 setback value #3

R30 setback value #4

R31 number of load capacitor values to be computed (no limit)

R32 C1

R33 C2 - values in pf

R34 C3 - one value must be entered for each

R35 C4 value of load capacitance specified in R31

. . - the values are used starting with R32

. .

. .

### Sample Output

Generate the voltage table for four setback levels  
and fire load capacitors.

#### Assume:

$$D_{33} = 350 \times 10^{-12} \text{ c/N}$$

$$\epsilon_o = 142 \times 10^{-12} \text{ c/cm v}$$

pz. .2" dia x .132" long

wt. .2" dia x .132" long

steel weight, density = .48 lb/cu in

#### Setback Levels

400 G's

600 G's

900 G's

1400 G's

#### Load Capacitor Values

0 pf

100 pf

150 pf

300 pf

470 pf

4.000 STO 19

.200 STO 20

.132 STO 21

.132 STO 22

350-12 STO 23

142-12 STO 24

STEEL

ASTO 25

.480 STO 26

400.000 STO 27

600.000 STO 28

900.000 STO 29

1400.000 STO 30

5.000 STO 31

0.000 STO 32

100.000 STO 33

150.000 STO 34

300.000 STO 35

470.000 STO 36

XEQ "TABLE"

#### OUTPUT VOLTAGE TABLE

PZ 0.200DIA X 0.132 IN

WT 0.200DIA X 0.132 IN

D33=350.0E-12 C/N

e.=142.0E-12C/CM V

STEEL WEIGHT

DENSITY=0.480 LB/CU IN

C. (pf)	G's	Vout
0	400	14.4
0	600	21.6
0	900	32.5
0	1400	50.5
100	400	6.7
100	600	10.0
100	900	15.0
100	1400	23.3
150	400	5.3
150	600	7.9
150	900	11.8
150	1400	18.4
300	400	3.2
300	600	4.8
300	900	7.2
300	1400	11.2
470	400	2.2
470	600	3.3
470	900	5.0
470	1400	7.8



# PROGRAM LISTING

<pre> PRP "TABLE" 01+LBL "TABLE" 02 27 03 STO 10 04 RCL 19 05 STO 13 06 RCL 31 07 STO 12 08 32 09 STO 11 10 XEQ 03 11 XEQ 04 12 XEQ 06 13 RTN  14+LBL 02 15 RCL 20 16 2 17 / 18 X12 19 PI 20 * 21 STO 15 22 RCL 22 23 * 24 RCL 26 25 * 26 RCL 17 27 * 28 9.80 29 * 30 .4536 31 * 32 RCL 23 33 * 34 STO 14 35 RCL 15 36 ENTER↑ 37 RCL 24 38 * 39 2.54 40 * 41 RCL 21 42 / 43 RCL 16 44 1 E-12 45 * 46 + 47 1/X 48 RCL 14 49 * 50 STO 18 51 RTN </pre>	<pre> 52+LBL 03 53 CLA 54 FIX 3 55 PRA 56 "OUTPUT VOLTAGE " 57 "TABLE" 58 PRA 59 CLA 60 PRA 61 "PZ " 62 ARCL 20 63 "DIA X " 64 ARCL 21 65 "I IN" 66 PRA 67 CLA 68 "WT " 69 ARCL 20 70 "DIA X " 71 ARCL 22 72 "I IN" 73 PRA 74 CLA 75 ENG 3 76 "D33=" 77 ARCL 23 78 "I C/N" 79 PRA 80 CLA 81 "e.=" 82 ARCL 24 83 "I C/CM V" 84 PRA 85 CLA 86 FIX 3 87 ARCL 25 88 "I WEIGHT" 89 PRA 90 CLA 91 "DENSITY=" 92 ARCL 26 93 "I LB/CU IN" 94 PRA 95 CLA 96 RTN  97+LBL 04 98 CLA 99 PRA 100 67 101 ACCHR 102 46 103 ACCHR 104 40 </pre>	<pre> 105 ACCHR 106 112 107 ACCHR 108 102 109 ACCHR 110 41 111 ACCHR 112 4 113 SKPCHR 114 71 115 ACCHR 116 39 117 ACCHR 118 115 119 ACCHR 120 5 121 SKPCHR 122 86 123 ACCHR 124 111 125 ACCHR 126 117 127 ACCHR 128 116 129 ACCHR 130 ADV 131 RTN  132+LBL 05 133 FIX 0 134 CLA 135 ARCL 16 136 ACA 137 CLA 138 6 139 SKPCHR 140 ARCL 17 141 ACA 142 CLA 143 6 144 SKPCHR 145 FIX 1 146 ARCL 18 147 ACA 148 CLA 149 ADV 150 RTN  151+LBL 06 152 RCL IND 11 153 STO 16 154 1 155 ST+ 11 156 XEQ 07 157 DSE 12 158 GTO 06 159 RTN  160+LBL 07 161 RCL IND 10 162 STO 17 163 1 164 ST+ 10 165 XEQ 02 166 XEQ 05 167 DSE 13 168 GTO 07 169 27 170 STO 10 171 RCL 19 172 STO 13 173 RTN 174 END </pre>
--	---	---

## DISTRIBUTION LIST

Commander  
U.S. Army Armament Research and  
Development Command  
ATTN: DRDAR-LCN-T (5)  
DRDAR-QAR-R  
DRDAR-TSS (5)  
Dover, NJ 07801

Administrator  
Defense Technical Information Center  
ATTN: Accessions Division (12)  
Cameron Station  
Alexandria, VA 22314

Director  
U.S. Army Material Systems Analysis Activity  
ATTN: DRXS-MP  
Aberdeen Proving Ground, MD 21005

Commander/Director  
Chemical Systems Laboratory  
U.S. Army Armament Research and  
Development Command  
ATTN: DRDAR-CLJ-L  
DRDAR-CLB-PA  
APG, Edgewood Area, MD 21010

Director  
Ballistics Research Laboratory  
U.S. Army Armament Research and  
Development Command  
ATTN: DRDAR-TSB-S  
Aberdeen Proving Ground, MD 21005

Chief  
Benet Weapons Laboratory, LCWSL  
U.S. Army Armament Research and  
Development Command  
ATTN: DRDAR-LCB-TL  
Watervliet, NY 12189

Director  
U.S. Army TRADOC Systems  
Analysis Activity  
ATTN: ATAA-SL  
White Sands Missile Range, NM 88002

Commander  
U.S. Army Armament Material  
Readiness Command  
ATTN: DRSAR-LEP-L  
Rock Island, IL 61299